Quaternary Science Reviews 214 (2019) 139–163

Contents lists available at ScienceDirect

Quaternary Science Reviews

journal homepage: www.elsevier.com/locate/quascirev

Ice-flow patterns and precise timing of ice sheet retreat across a dissected fjord landscape in western Norway

Jan Mangerud [a, b, *], Anna L.C. Hughes [a, b, c], Tone Herfindal Sæle [a, b], John Inge Svendsen [a, b]

[a] Department of Earth Science, University of Bergen, PO Box 7803, 5020, Bergen, Norway
[b] Bjerknes Centre for Climate Research, Bergen, Norway
[c] Present address: Department of Geography, School of Environment, Education and Development, The University of Manchester, Manchester, M13 9PL, UK

ARTICLE INFO

Article history:
Received 7 February 2019
Received in revised form
23 April 2019
Accepted 29 April 2019
Available online 17 May 2019

Keywords:
Scandinavian ice sheet
Fennoscandian ice sheet
Ice-margin retreat rates
Glacial striae
Glacimarine terraces
Ice-berg calving
Glaciology
Scandinavia
Glacial geomorphology

ABSTRACT

We reconstruct patterns of ice flow and retreat of the southwestern Scandinavian Ice Sheet, from 2900 field observations of glacial striae and elevation measurements of 60 ice-marginal-deltas from a high-resolution LiDAR DEM. During the Last Glacial Maximum, ice flow was towards the west across the entire area, including across several-hundred meter deep north-south oriented fjords. During deglaciation, ice flow adjusted to topography and the dominant flow direction switched towards the southwest. We use a shoreline diagram constructed from relative sea-level curves to establish the age of each delta, which allows us to constrain the timing of retreat with almost decadal precision. Rapid ice sheet retreat commenced at the onset of the Holocene at 11,600 cal years BP. Retreat rates were 160 m a^{-1} in the deepest fjords, 60–80 m a^{-1} in shallower fjords, and even slower for land-terminating margins. The fastest retreat rates, 240 m a^{-1} and 340 m a^{-1}, were experienced in the largest fjords, Hardangerfjorden and Sognefjorden, which border the study area to the south and north. Crosscutting glacial striae indicate that calving bays developed during retreat along the widest fjords. The combination of complex fjord topography with fast ice-margin retreat by iceberg calving, led to isolation of ice remnants on islands and peninsulas, a process that accelerated the overall rate of deglaciation. Ice-margin retreat paused between 11,300–11,100 cal years BP, probably due to cooling during the Preboreal Oscillation.

1. Introduction

In this paper, we address three research questions: 1) How, in detail, does ice sheet flow occur across a landscape with several-hundred-metre-deep fjords oriented parallel, obliquely and at right angles to the main ice-flow direction? 2) How does ice-flow change as the ice sheet retreats and thins in such a landscape? 3) What was the pattern and chronology of ice-margin retreat across such a landscape in western Norway?

The results give insights into processes and mechanisms for retreat of ice sheets through landscapes of complex topography and large variations in relief, in particular the balance between retreat on land and through deep fjords. Results also provide an empirical description of how fast this western sector of the Scandinavian Ice Sheet retreated during the abrupt and large-amplitude climate warming at the onset of the Holocene, a scale and rate of climatic transition that is somewhat comparable to projected near-future warming (IPCCP, 2014). The dissected fjord landscape of western Norway is an apt analogue for complex coastal fjord regions at the margins of the Greenland Ice Sheet. Our results are also crucial to understand patterns and timing of immigration of plants, animals and humans that now could enter this area for the first time in more than 30,000 years (Mangerud et al., 2011).

Glacial striae found on bedrock surfaces record ice-flow directions at the base of the former ice sheet. In the area around Bergen, western Norway, there are several-hundred-metre deep fjords oriented in almost all directions, including perpendicular to reconstructed ice-flow directions of the former Scandinavian Ice Sheet during its maximum extent (Vorren, 1977; Kleman et al., 1997) (Figs. 1 and 2). The area is therefore suitable for studying past ice-flow directions at the base of a thick ice sheet and if the flow pattern followed or ignored major topographic features such

* Corresponding author. Department of Earth Science, University of Bergen, PO Box 7803, 5020, Bergen, Norway.
E-mail address: Jan.Mangerud@uib.no (J. Mangerud).

https://doi.org/10.1016/j.quascirev.2019.04.032

Abbreviations

BP	calibrated radiocarbon years Before Present (=1950)
LGM	Last Glacial Maximum
YD	Younger Dryas
ELA	Equilibrium Line Elevation
N	north
NNE	north-northeast, etc.

as fjords and mountains. We present some 2900 measurements of glacial striae, which together show how the ice margin and ice-flow directions adjusted to the underlying topography during the last deglaciation.

Analyses of glacial striae provide useful information to reconstruct the pattern of the deglaciation, but can only provide information on the relative timing of changing ice-flow directions and ice-margin positions. In order to constrain the absolute timing of ice sheet retreat, we construct a well-dated shoreline diagram and use this to assign absolute ages to ice-marginal deltas and other marine terraces that formed in front of the retreating ice margin. The shoreline diagram is based on multiple isolation basins and numerous radiocarbon dates, and allows us to determine the age of ice-marginal deltas with almost decadal precision. Combining the information from glacial striae and dated ice-marginal marine terraces, we have been able to reconstruct the retreat of the Scandinavian Ice Sheet through the dissected fjord landscape of western Norway with unprecedented precision.

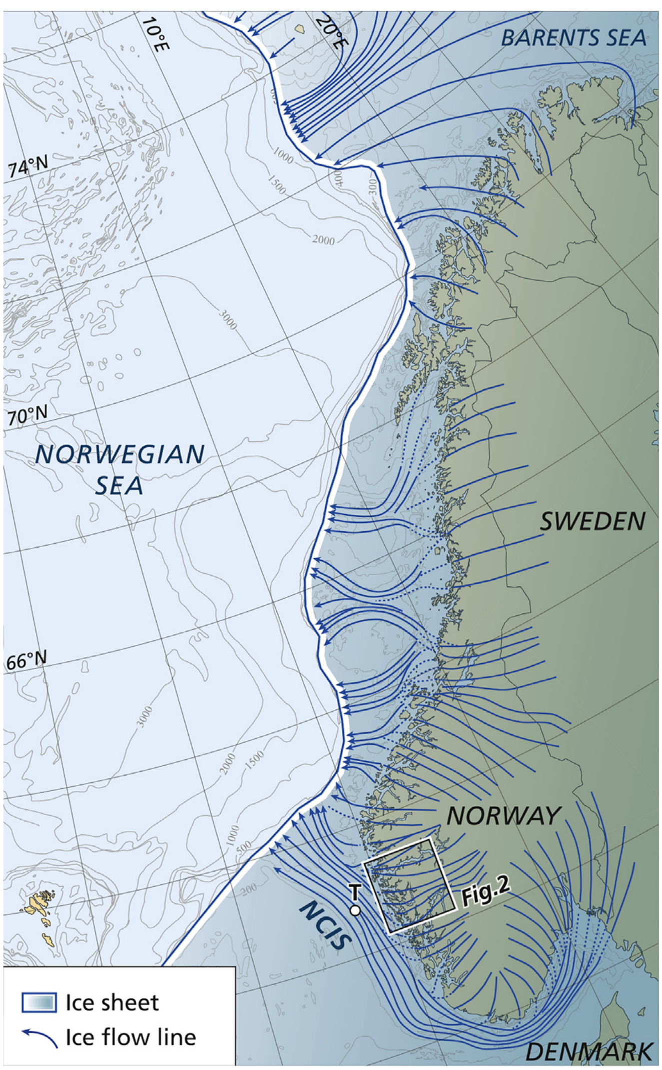

Fig. 1. The western part of the Scandinavian Ice Sheet. NCIS – Norwegian Channel Ice Stream. T – Troll core. Box shows Fig. 2. Modified from Vorren and Mangerud (2008) and Ottesen et al. (2005).

2. Regional setting

The study area is located between Hardangerfjorden and Sognefjorden, the two longest fjords in Norway (Figs. 1 and 2). Much of the bedrock in this region belongs to the so-called Bergen Arcs that include Silurian shales and limestone formations layered between harder volcanic and crystalline rocks (Fossen et al., 2008; Kolderup and Kolderup, 1940). Fjords, valleys and mountain ridges follow these large-scale-arcuate bedrock structures (Fig. 2). The fjord systems Bjørnafjorden-Fusafjorden and Fensfjorden, and lakes on Osterøy, comprise the outer arc. The innermost arc includes the valley where the city of Bergen is located. There are often separate names for different parts and sub-branches of Norwegian fjords, but here we have simplified the naming; for example, our Fusafjorden includes Fusafjorden, Eikelandsfjorden, Ådlandsfjorden, Samnangerfjorden and Trengereidfjorden.

The islands to the west of the Bergen Arcs (Sotra, Øygarden, Askøy) and the mountains surrounding the Bergen Arcs consist of Precambrian crystalline rocks, mainly granites and gneisses. North-south oriented faults and fracture zones crosscut all bedrock formations in the region, and some fjords and valleys follow these fractures; for example 390-m-deep Veafjorden. All fjords contain several tens of metres of post-glacial sediments (Aarseth, 1997), mainly glacimarine silt and clay, and thus the real depth to bedrock is larger than the given water depth. The terrestrial landscape of the study area is dominated by exposed bedrock, except for some restricted areas that are covered by ice-margin deposits or bogs. Because of the general lack of Quaternary (unconsolidated) sediments, there are almost no wave-formed shorelines, not even along the exposed western seaboard.

Two main fjord systems, Korsfjorden in the south and Fensfjorden to the north, cross through the western row of islands and therefore, at least in some periods, probably served as primary drainage channels for glacial ice, although both have shallow sills near their mouths. Korsfjorden is 610 m deep to the south of Sotra, but two km west of the islands, the maximum depth is 260 m. Fensfjorden is more than 650 m deep for a distance of more than 10 km, but only about 300 m deep where it crosses the westernmost islands.

During the Last Glacial Maximum (LGM) the Scandinavian Ice Sheet covered the entire study area; the ice divide was located in the mountains far to the east (Fig. 1) (Kleman et al., 1997) and the western ice margin met the British Ice Sheet in the North Sea (Sejrup et al., 2016). At this time, the main ice-flow direction was from east to west across the entire area. During late phases of the LGM, between about 24,000 and 19,000 BP (Becker et al., 2017) the Norwegian Channel Ice Stream flowed northwards shortly outside the coast (Fig. 1). Glacial lineations on the inner shelf show that ice-flow from land turned towards north, into the Norwegian Channel Ice Stream (Ottesen et al., 2016), which was the primary drainage route for ice from our study area until break-up of the ice stream after 19,000 BP (Sejrup et al., 2016; Svendsen et al., 2015a,b).

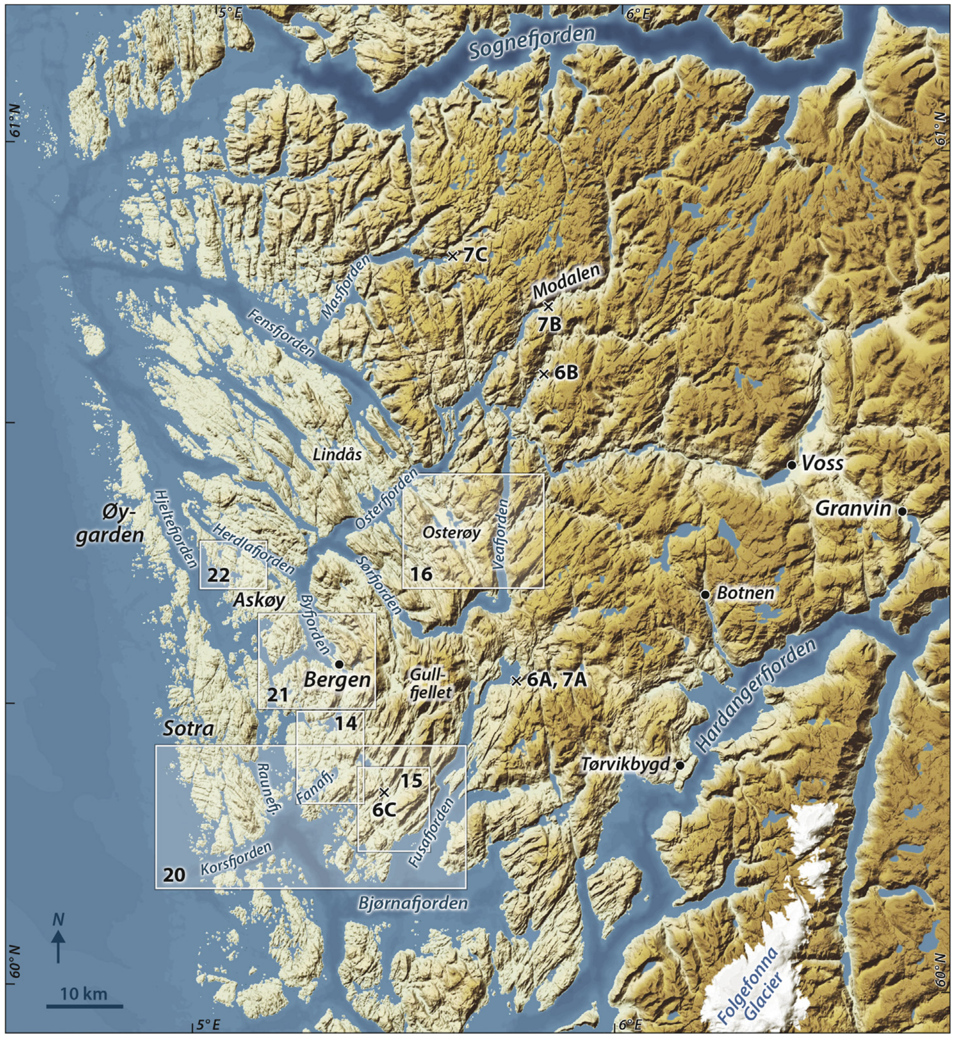

Fig. 2. Overview map of the study area and surroundings. For location, see Fig. 1. The (Fig.-) numbered frames show location of maps and crosses show location of Figs. 6 A, B, C and 7 A, B, C.

3. Methods and materials

3.1. Glacial striae

Analysis of glacial striae has a long tradition in the Nordic countries and JM learned the methods mainly by field training with Just Gjessing, Per Holmsen and Hans Holtedahl. The methods are documented in Ljungner (1930) and Gjessing (1953) and in recent textbooks (e.g. Benn and Evans, 1998). Glacial striae are in this area common in the tidal zone because of the ongoing emergence and that basic seawater reduces bedrock weathering compared to more acidic rainwater (Fig. 3A and B). Soils in western Norway are acidic and above sea level striae are mainly found on quartz lenses or other weathering-resistant rock types (Fig. 3E), or at sites that have been covered by till or other sediments and recently exposed. The most important features for determining relative ages of crossing glacial striae have been stoss and lee sides (Fig. 3C) of often small, mm-sized irregularities, partly inside striae or in the lee of small quartz lenses.

We collected glacial striae mainly from Master theses and field notebooks in a database (Table S1; Fig. 4 and Fig. S1); references are given in Table 2. Some, but far from all, of these observations are published (Aa and Mangerud, 1981; Aarseth and Mangerud, 1974; Hamborg and Mangerud, 1981; Mangerud, 1970; Mangerud and Skreden, 1972). The database is described in *Suplemental online material.*

The collated striae were then used to reconstruct former ice flow patterns and the retreat pattern (Gjessing, 1953; Kleman, 1990). It is generally accepted that most preserved glacial striae are formed close to the ice margin and thus record the ice-flow direction close to the ice sheet edge (Gjessing, 1953; Kleman, 1990). This means that the pattern of ice-margin retreat can be reconstructed by measuring glacial striae and assuming that the ice margin was oriented perpendicular to the youngest striae. However, crosscutting striae and the survival of Allerød (Mangerud et al., 2016) and even Eemian sediments (Mangerud et al., 1981) that were overrun by the Younger Dryas (YD) ice, show that some striae in this area may be older than the deglaciation. Nevertheless, we assume that the vast majority of striae were formed shortly before the area became ice-free; an assumption supported by the pattern of striae directions. A main criterion for correlating striae in order to reconstruct ice-flow patterns is that the used directions and relative ages are internally consistent.

Fig. 3. Photos of glacial striae. Arrows show flow direction.
A. Striae 260° on a steep slope at sea level in Kjekallevågen (No. 2669, Table S1).
B. Whalebacks with clear striae, a common feature in this area. Fensfjorden (No. 2662, Table S1).
C. Cross-cutting striae along the shore of Hetleflotvatn (Fig. 15). The knife shows the youngest striae, towards 110°. The light-greenish brush shows orientation of older striae 166° in a lee side. The pencil (136°) and magnifying glass (114°) show some intermediate directions. (Nos. 1074–1078, Table S1).
D. Striae 942 m a.s.l. on Gullfjellet, Bergen (Table S1, No. 2641). Ski poles are 1.3 m long. Such striae in the mountains are found only on resistant bedrock. The lee side is a 200 m high wall.
E. Glacial striae on a quartz lens, where the surrounding bedrock is weathered. Typical example from mountain areas. On Flatafjell west of Veafjorden (Figs. 16), 600 m a.s.l. (No 2202, Table S1).

3.2. Dating ice-margin positions with a shoreline diagram

All referred radiocarbon dates are cited from published papers and all ages are given as calibrated radiocarbon years Before Present (=1950, hereafter only BP) according to IntCal13 (Reimer et al., 2013). We emphasize that although we date marine landforms, all cited dates used for the shoreline diagram are derived from terrestrial plant macrofossils (section 3.2.1) and thus no marine-reservoir-age corrections are involved or necessary.

An ice-marginal delta represents the local sea-level altitude at the time the ice margin was located at the delta. This means that if the age of the paleo-shoreline at the time of the delta formation can be determined, then both the ice marginal delta, and the corresponding position of the ice margin, can be dated (Aa and Mangerud, 1981; Hamborg, 1983; Romundset et al., 2017; Sørensen, 1979). The relative sea level was, in the studied area, falling 3–10 m per 100 years during the deglaciation period, due to rapid glacio-isostatic uplift and decreasing gravity of the diminishing ice sheet. The pattern of isostatic uplift also caused a strong tilting of the shorelines in western Norway, about 1.3 m km^{-1} for the YD shoreline (Aarseth and Mangerud, 1974; Lohne et al., 2007). The implication is that in this region ice-marginal deltas that formed 100 years apart will have an altitude-difference of up to 10 m. The paleo-sea level corresponding to a particular ice marginal delta can be determined with a precision down to one meter in favourable situations where the delta surface is well preserved. Our dating procedure consists of five steps.

3.2.1. Step 1. constructing relative sea-level curves

All ages are based on relative sea-level curves that were constructed by using the isolation-basin method, where the transition between marine and lacustrine sediments were radiocarbon dated using terrestrial plant macrofossils. We use a slightly modified version of the well-dated (>50 ^{14}C dates) relative sea-level curve from the island Sotra (Fig. 2) where emergence was slow (Fig. S2) (Lohne et al., 2007). This was combined with another curve from Tørrvikbygd, about 60 km farther east (Fig. 2), where emergence was significantly faster (Fig. S3) (Romundset et al., 2010). Construction of the two sea-level curves are described in *Suplemental online material* with the determined elevations per century given in Table S2.

3.2.2. Step 2. determining the direction of isobases

The real tilt of a shoreline can be measured only at right angles to the uplift isobases. Our isobases are mainly determined by measuring the height of a number of ice-margin deltas that were formed during a relative-sea-level high-stand at the end of the YD. The YD deltas define the 3-dimensional configuration of the corresponding shoreline, which is now tilted 1.3 m km^{-1} due to glacioisostatic uplift (Aarseth and Mangerud, 1974). For most of the study area we use a slightly modified isobase-direction of 351° after Lohne et al. (2007), but north of Herdla the isobases bend eastwards and here we follow the original direction measured by Aarseth and Mangerud (1974). We notice that this slight curvature of the isobase-direction introduces an uncertainty of some few decades when dating the marine limits in the northernmost area. We postulate that the isobases-direction did not change during the deglaciation period and that shorelines in the diagram can be considered as straight lines, although we realize that they must have been slightly curved and flattened out towards the ocean in the west and the uplift centre in the east. However, since we study only a relatively short segment, maximum 100 km in length, we consider that any bending of the shorelines is negligible for our study area. We project all observations, such as the relative sea-level curves and altitudes of ice-margin deltas, along the isobases into a vertical plane oriented perpendicular to the isobases.

3.2.3. Step 3. construction of a master shoreline diagram

We then identify the altitude of relative sea level at a certain time in both sea-level curves, e.g. at 11,000 BP, and draw a straight line between the two points. This line represents the 11,000 year-old shoreline. In practice, we draw a line every 100 years during the deglaciation period (Table S2). The master shoreline diagram constructed this way is shown in Fig. S4 and parts of it in Fig. 5.

3.2.4. Step 4. determining the altitudes of ice-marginal deltas

Most of the sites we use (Table 1) have been described before (Aa and Mangerud, 1981; Hamborg, 1983; Kolderup, 1908; Skreden, 1967). However, these authors measured different parts (proximal, distal, etc.) of the terraces, used different measuring methods, and they applied different reference levels. We have therefore re-measured the altitude of all 60 terraces from Digital Terrain Models (DTM) derived from LiDAR data compiled by the Norwegian Mapping Authority (https://hoydedata.no/LaserInnsyn/), which uses the Norwegian Normal zero (NN2000) as a datum; in practice mean sea level. From this DTM-data altitudes can be determined with a precision of less than 10 cm. Examples of terraces on hill-shaded renditions of the DTM data are shown in Fig. 6 and photos in Fig. 7. Where possible we have measured the distal part of the terraces, which we consider reflects contemporaneous sea level best. This should give a consistent dataset and we assume these altitudes reflect the mean paleo-sea-level. A major problem, in addition to natural irregularities, is that in several places most of the deposits have been exploited for sand and gravel and thus the distal parts of the deltas have been removed. We have examined all terraces in the field. Ideally, one should measure the elevation of the boundary between the foresets and topsets, but most gravel pits are now closed and very few sections are available.

Most terraces have a distinct ice-contact slope, and almost all consist of glacifluvial gravel. Some very few (Table 1) cannot be directly related to an ice margin, but because the emergence was so fast, all marine limit terraces must have been formed close to the ice margin and at least show that the site was ice-free at the time of the corresponding sea level.

3.2.5. Step 5. dating ice-margin deltas and other marine limit terraces

The final step is to plot the ice-marginal deltas on the master shoreline diagram to obtain their age. We use the map position of the 40-m-YD shoreline isobase as the zero line for distances along the transect (Fig. 9). Ice-marginal deltas are projected along the isobase-direction and plotted according to altitude (m a.s.l.) and distance from the 40-m-YD isobase, measured at right angles to the direction of the isobases. Then we read the age of each delta from the shoreline diagram (Figs. S4 and 5). For terraces located between each 100-year interval, we simply interpolate the age from the plot. In Fig. 8 we present an example of the results of this process. We note that we use the Younger Dryas as a chronostratigraphic/geochronologic unit with boundaries defined by climatic changes in southern Scandinavia (Mangerud et al., 1974) and with the presently best age estimates of the boundaries in calibrated C-14 years of c.12,740–11,540 BP (Lohne et al., 2013, 2014).

It is difficult to calculate and combine all errors (isobase-direction, tilt of shorelines, errors in radiocarbon dates, estimated ages in relative sea-level curves, etc.) mathematically, but we estimate that total accumulated uncertainties are of the order of 100 years for the absolute age of the ice margins. However, we consider that the error in estimated age-differences between closely spaced ice-margin positions often are less than 20 years and this difference, which give the ice-margin retreat rate, is of most interest for this paper. The C-14 plateau at the end of the YD is a main source of error in the absolute numerical age value, but both the onset of ice-margin retreat at 11,600 BP (Lohne et al., 2012) and the onset of the emergence at 11,550 BP (Lohne et al., 2007) are dated with a series of dates across the plateau. The small error for the age differences is because they are calculated from emergence rates and altitude differences for terraces (Fig. 8). A time difference of 20 years corresponds to a height difference of 2 m across much of the area and we consider that we have determined the terrace elevations and corresponding sea level with better precision. The LiDAR-derived digital elevation model has a horizontal resolution of 1–2 m and a vertical resolution of 10 cm or better.

3.3. Searching for moraines

Much of the area has been systematically investigated for other ice marginal landforms and sediments (e.g. Aa and Mangerud, 1981; Aarseth and Mangerud, 1974; Hamborg and Mangerud, 1981; Skreden, 1967) using air photos and field work. Short moraines and other ice-margin deposits are found here and there, especially in the valleys, but no moraines inside the YD limit could be traced for any distance or correlated to reconstruct an ice margin with certainty. We re-examined the entire area using hill-shaded renditions of high-resolution (1–2 m) DTMs constructed from LiDAR data (section 3.2.4). However, we still did not find any clear moraines that could be traced across large distances. Thus, our

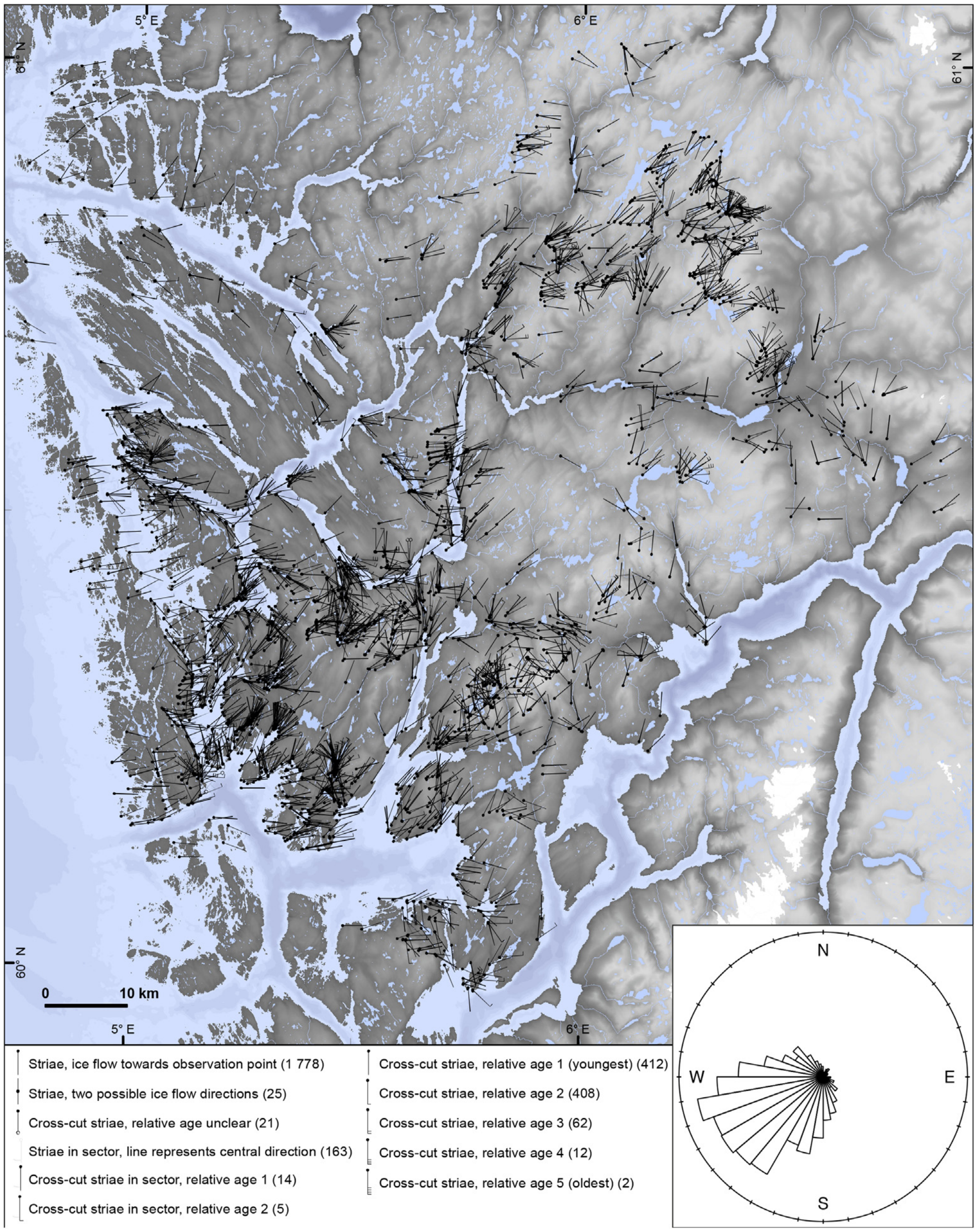

Fig. 4. Map showing all glacial striae listed in Table S1. The rose diagram shows the striae plotted in 10° sectors. Fig. S1 is a high-resolution A0-size pdf version of this map including elevation contours. Numbers in brackets show number of observations of each type.

reconstruction of the retreating ice margin is based entirely on the dating of marine terraces and the patterns of ice flow recorded by observations of glacial striae.

4. Results and interpretation

4.1. Ice-flow directions

All glacial striae are plotted in Fig. 4 and in a high-resolution pdf file so that the reader can zoom in and see details of both topography and location of striae (Fig. S1). Some striae are presented on more detailed maps. The bulk of striae show ice flow in a wide sector around the WSW, reflecting the general slope direction of the landscape. The large overall spread, including S-E and N-E directions, reflects more variable ice flow directions as deglaciation progressed. For example, as ice retreated from the deep fjords, ice from adjacent high ground flowed towards these fjords, partly along valleys and inlets.

4.2. Shoreline diagram and the age of ice-margin terraces

The constructed master shoreline diagram that we use for dating the terraces is given in Figs. S4 and Fig. 5. The individual terraces are described in Table 1. The ages for the deglaciation of each terrace site, as deduced from the shoreline diagram, are given in Table 1 and plotted in Fig. 9.

4.3. Pattern and timing of the deglaciation

We have produced a series of maps showing the changing ice flow and the pattern and timing of retreat (Figs. 10–13) based on the measured glacial striae and our dating of ice-margin terraces.

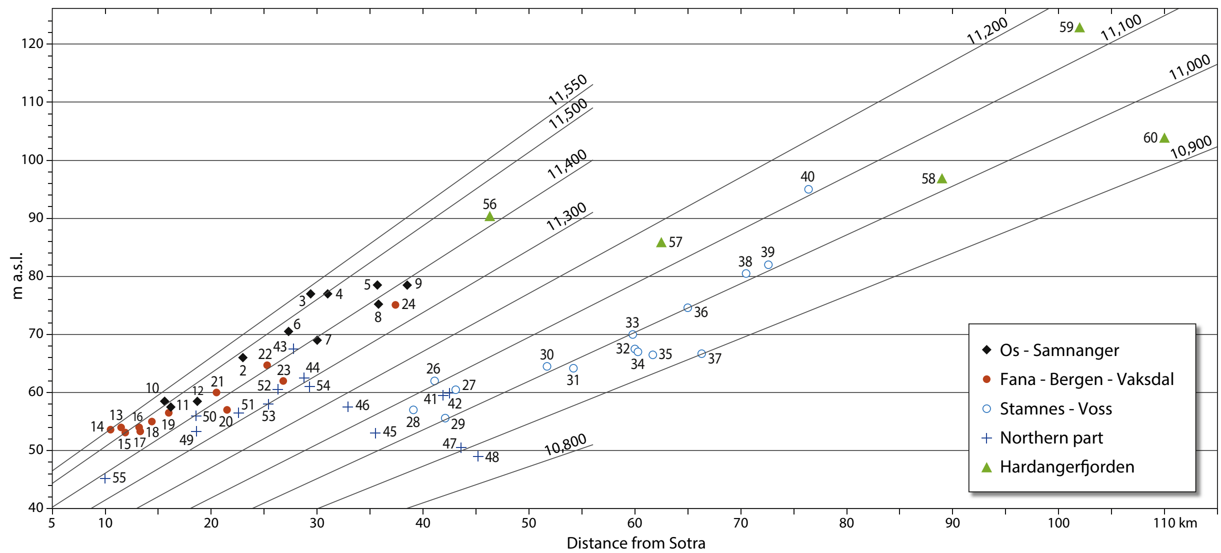

Fig. 5. A part of the master shoreline diagram with extrapolated lines to 115 km. All measured marine-limit sites proximal to the Younger Dryas moraine are plotted. The signs represent a geographical grouping. Some sites (limited by space) are numbered; locations are shown on the map Fig. 9 and details given in Table 1.

We will here present the deglaciation maps and shortly explain the basis for each reconstruction. We have in areas without dated terraces drawn simple, almost straight lines for the ice margin, at right angle to the direction of glacial striae, but without consideration of the topography, the difference can be seen by comparing the mapped Eidfjord-Osa moraine in Fig. 13 with lines north of Hardangerfjorden in Fig. 12. We discuss some principal questions arising from the reconstruction in later sections.

4.3.1. *Reconstruction of the ice sheet at 20,000 BP*

We postulate that the westernmost observed striae, found on low skerries and islands along the outermost coast, record the oldest ice-flow directions in the study area. These striae show ice-flow towards the west or slightly south of west and their directions are similar to the directions of sea-floor glacial lineations mapped only some 6–8 km further west and which turn north into the Norwegian Channel Ice Stream (Ottesen et al., 2016) (Fig. 1). Thus, these oldest striae may give the landward picture of ice flow during the period that the Norwegian Channel Ice Stream operated. However, as discussed in the next section, we find it more probable that the striae on the outermost islands were formed at a later stage, after the retreat of the ice stream, when the ice margin was located shortly outside the outermost islands. We tentatively correlate some east-west orientated striae found inland with the striae found at the coast (section 4.3.2). This interpretation is based on the facts that these striae are found at the highest summits, show no concordance with large variations in local topography, and are the oldest where cross-cutting striae are observed (Fig S1). Independent of the real age of the measured striae, we consider that the ice-flow pattern shown by these striae may be representative for several phases of the ice sheet.

4.3.2. *Reconstruction of the ice sheet at 15,000 BP (Fig. 10A)*

The margin of the Norwegian Channel Ice Stream had retreated to south of our area by 18,500 BP (Morén et al., 2018; Sejrup et al., 2009). However, the islands along the coast did not become permanently ice-free until about 14,800 BP (Mangerud et al., 2017). This means either that the ice margin was located on the inner part of the continental shelf for almost 4000 years or that the ice margin retreated inland and re-advanced beyond the coast again before 14,800 BP. Independent of these alternatives, we find it most likely that most of glacial striae on the outer islands were formed near the ice margin shortly before deglaciation of the outer coast at 14,800 BP and we apply the age 15,000 for this stage in our reconstruction. Their directions show that the ice margin was parallel with the coast (Fig. 10A). There are some small variations in directions of these westernmost striae; some instances of cross-cutting suggest that due west is the oldest and that the direction slightly south of west is younger, suggesting minor adjustments in the ice flow before retreat.

It is impossible to robustly correlate these westernmost located striae with striae further inland. However, glacial striae on high and freely located mountain summits must record ice-flow directions when the ice was thick enough to cover these summits as a minimum. We therefore assume that such striae will provide a general picture, although not a synchronous snapshot, of ice-flow directions when the ice margin was located beyond, or close to the outermost coast. That these striae record a regional ice flow pattern when the ice was thick enough to cover the highest mountain summits in the study area is reinforced by observations of E-W orientated striae on summits on either side of deep and narrow fjords orientated N–S (Fig. 16). Glacial striae on the mountains on Sotra, which reach up to 340 m a.s.l. and are located only 10–12 km east of the westernmost striae, show similar westerly ice-flow directions and were probably formed simultaneously with the westernmost striae. The westernmost mountain reaching close to 1000 m a.s.l. is Gullfjellet, located only 35 km inland (G in Fig. 10A). Striae on two summits on this mountain, at 960 and 980 m a.s.l., located about 4 km apart, all show directions due west (Table 1, Fig. 3 and Fig. S1) and were probably formed when the ice margin was located beyond the coast.

There are more variations in striae directions on mountain summits further inland (Fig. 4 and Fig. S1) and some may stem from younger periods. However, the highest, and presumably oldest striae, everywhere show ice flow independent of valleys and other local topography and thus reflect an ice-sheet surface well above the highest mountains. We have not attempted to resolve different phases of flow of the thick ice, but we are surprised that such topography-independent striae are preserved on so many summits. Part of the explanation may be that the ice became cold-based as the ice became thinner, and thus preserved these older striae.

We conclude that the ice flow was almost parallel, independent

Table 1
Description of the terraces.

Site no	Site	Lat. **N** EU89	Long. **E** EU89	Dist.[a] Km	Distal part of terrace. m a.s.l. From	To	Refs.[b]	Age[c]	Comments
1	Ulven, Os	60.1925	5.422	14		59.0		11550	A large ice-marginal delta (Aarseth and Mangerud, 1974) used for construction of isobases (Lohne et al., 2007).
2	Lønningdal	60.2689	5.561	23	65.0	67	64[K] 64[H]	11480	There are terraces all around the short valley between Øvretveitsvatnet and the sea, but we conclude the valley was not filled with sediments up to the marine limit. Most sediments apparently came out Stordalen (i.e. from NE), but some also from the small valleys on the opposite side.
3	Hafskår	60.2476	5.6845	29.4	76.5	77.5	76[H]	11540	Most of the terrace is eroded away by the river; remnants of the highest part are less than 100 m in length.
4	Ådland	60.2889	5.6915	31	76.0	78	76[H]	11500	Here are terraces in a narrow valley with sloping terraces, so it is difficult to determine palaeo-sea level.
5	Skjeldbred, Eikelandsosen	60.2486	5.7958	35.7	78.4	78.6	77,6[K]	11440	A distinct ice-marginal delta, 300 × 200 m in area and with a 3 m-high moraine ridge sitting on the terrace.
6	Rolfsvåg	60.3291	5.616	27.3	70.0	71.0	70[H]	11470	A well-defined glacifluvial-river delta that was deposited from the Gullfjellet mountain massive. The terrace, covering an area of about 200 × 200 m, is dissected by the river and a gravel pit. We measured two remnants of the original delta surface, each about 80 m across. In the gravel pit the steepest, boulder-rich foresets are dipping 30°, whereas most beds are dipping 20–25°. It is estimated that the topset is about 1 m thick.
7	Nordbø, Samnanger	60,3840 60.3809	5,6455 5.6442	30	68.0	70.0	75[H]	11390	A long, but very narrow terrace as well as a small terrace, 80 × 50 m, were measured. They were probably formed by wave action in water-saturated till soon after the deglaciation. Thus this terrace was formed by different processes than almost all the others.
8	Tysse, Samnanger	60,3741 60,3730	5,7638 5,7589	35.8	75.2		75.2[K] 76[H]	11390	Ice-marginal delta that we assume has filled the narrow river valley. There is a well-defined terrace, 100 × 50 m, on the north-eastern side of the river, which is the highest remnant of the palaeodelta. A very distinct terrace (80 × 50 m) south-west of the river is 73–74 m a.s.l. and its location is indicated with the second set of co-ordinates.
9	Svendsdalen, Samnanger	60.3879	5.8019	38.5	78.3	78.6	81[H]	11380	This is a small, but well defined terrace that forms the foundation of a small cabin next to the steep valley side. The terrace is only 20 m across, but considered to be a reliable marine limit. The measured marine-limit altitude is supported by several other small terraces in the vicinity (Hamborg, 1983).
10	Hetlefloten	60.2157	5.441	15.6	58.0	59.0	58,4[K]	11530	Ice-marginal delta 200 × 300 m. Steep dipping gravel foresets capped by topset were exposed in a pre-existing gravel pit.
11	Søfteland	60.2413	5.4453	16.2	57.5		58,7[K]	11480	An ice-marginal delta has filled the entire valley for a distance of c 1.5 km, but the deposit is subsequently dissected by the river. The measured terrace is c 150 × 100 m and the surface is horizontal. The topset is 1–1.5 m thick and the foresets are dipping 20–30°, in a now closed gravel pit.
12	Gåssand	60.2578	5.4847	18.7	58.0	59.0		11440	Ice-marginal deposit, about 100 m wide and 500 m long, located in front of the deep lake Rødlivatnet. Most of the present surface is sloping, mainly due to subsequent erosion. We consider a distinct flat part (58–59 m a.s.l.) next to the old farmhouse to represent the marine limit.
13	Fana	60.2618	5.3526	11.5	53.7	54.2	53,5[K]	11530	This is a large ice-marginal delta where a lake marks the ice-contact slope.
14	Stend	60.2745	5.327	10.5	53.4	53.9	54[K]	11550	Ice-marginal delta some 0.5 km long. Earlier there was a distinct ice-contact slope at the NE end, facing Rådalen; that is now removed by infilling. The surface of the terrace is disturbed several places by digging, etc.
15	Skjold	60.3083	5.3377	11.9	52.8	53.4	52[K]	11500	The terrace, some 200 × 200 m in area, is now an urban area, but still distinct. It was formed as an ice-marginal delta. The old gravel pit can be seen as slopes.
16	Elveneset, Nesttun	60.3102	5.3636	13.2	53.8	54.2		11480	This is a small distal remnant of an ice-marginal delta, which was removed because of house construction. Foresets showed that it was deposited from (south) an ice lobe filling Birkelandsvatnet.
17	Øvsttun	60.316	5.363	13.3	52.8	53.8	53,6[K]	11470	Most of this ice-marginal delta is removed or covered by buildings.
18	Årstad, Bergen	60.3811	5.3586	14.4	54.0	56.0	56,4[K]	11490	Kolderup (1908) measured the inner part of the terrace. The terrace is now an urban area. In 2009 we measured the boundary between foresets and topsets to 53.2 m a.s.l. during a construction site excavation, but parts of the topsets were removed.
19	Jordalen	60.4269	5.3636	16	56.0	57.0		11450	Small terrace on both sides of the creek.
20	Indre Arna	60.3925	5.471	21.5	57.5	58.5	60,5[K]	11370	This is the flat valley floor located only 1–2 m above the river.
21	Mjeldheim, Arna	60.4193	5.4593	20.5	59.5	60.5	54,9[K]	11430	Much of the terraces are removed by gravel pit activity, but there are remnants, some 40 × 20 m on both sides of the river.
22	Mjelde, Osterøy	60.4535	5.5347	25.3	64.4	65.0	65[A]	11400	Distinct marine-limit delta. The measured terrace is c 100 × 100 m and very flat.
23	Gjerstad kirke, Osterøy	60.5002	5.547	26.8	61.5	62.5	63,2[K]	11450	About 200 m long terrace along the small river.
24	Vaksdal	60.4813	5.75	37.4	74.6	75.6	68,2[K] 68[A]	11350	Kolderup (1908) apparently measured the terrace close to the fjord, presently covered by the main village of Vaksdal. We measured a terrace at Sanddalen about 1 km up-valley. It is some 400 × 200 m in area, sloping very slightly from the river mouth into the bay of the valley where it is located. Two small sections, only ~1.5 m deep showed sorted sand and gravel. According to local people, there have been large gravel pits in the front. The 25 m high back wall of the pits, overgrown by small trees, can still be seen. We consider this to be a safe marine limit.
25	Helle, Stanghelle	60.5662	5.7604	39.7	57.0	59.0	62,6[K] 61[S]	10980	Ice-marginal marine deposits cover the bedrock, but no well defined terrace. Sharp upper limit of deposits at 59 m, but Marin Limit might be higher.
26	Dalegarden, Dale	60.5771	5.7948	41.1	60.0	64.0		11110	Ice-marginal deposit along the valley side. Top surface, about 100 × 100 m is not horizontal. Gives approximate height of marine limit only.
27	Dale	60.5899	5.82	43.4	59.0	62.0	51,6[K] 65[S]	11060	The village of Dale covers the entire terrace, but we still consider the measurements as precise. The top point is 65 m a.s.l. The main terrace is 400 × 300 m.

Table 1 (*continued*)

Site no	Site	Lat. **N** EU89	Long. **E** EU89	Dist.[a] Km	Distal part of terrace. m a.s.l.		Refs.[b]	Age[c]	Comments
					From	To			
28	Stamnes	60.6658	5.752	39.1	56.5	57.4	56,8[K] 57[A]	11060	Ice marginal delta dissected by deep ravines. The top surface is about 0.5 km across.
29	Straume	60.6544	5.8082	42.1	55.2	56.0	57[A]	11000	Ice-marginal delta that originally has been about 0.5 km long. Our altitude is measured in the flat proximal part. A ravine cuts through the entire terrace and on the other side of the ravine the terrace is 56.5–57 m a.s.l. (60.6562 N, 5.809 E), measured by Aa and Mangerud (1981), but we consider it may have a cover of sloped sediments.
30	Flåti, Bolstad	60.6362	5.9561	51.7	64.0	65.1	64[K] 62[S]	11020	Distinct terrace, 150 × 100 m. Clear marine limit.
31	Horveid, Bolstad	60.6507	5.9941	54.2	64.0	64.5	63[S]	10980	Large ice-marginal terrace, 500 × 100 m. Well preserved, almost horizontal surface, but tilting from 65 m a.s.l. near the river to 64 m a.s.l. into the tributary valley.
32	Teigdalen, Evanger	60.663	6.0922	60	67.0	68.0	67,1[K]	10960	Narrow terraces along the valley slope. Some 200 m long, but less than 20 m wide.
33	Fadnes, Evanger	60.6567	6.0932	59.8	68.0	72.0	65[K] 67[S]	11050	Ice-marginal delta. Foresets show it was deposited from the tributary valley. Almost removed by gravel pit. Presently no distinct top surface.
34	Solviki, Evanger	60.6533	6.101	60.3	67.5	68.5		10970	Small but clear terrace, only about 100 m long and 30 m wide. Thick cover of till above the terrace, so it might have been formed by down-washed material.
35	Skorve, Evanger	60.6476	6.1329	61.7	66.4	66.7		10940	Small terrace, only some 10 × 30 m. We would not trust this alone, but it generally support the measurements of the other terraces.
36	Geitle	60.6393	6.202	65	74.3	74.9	74[S]	10990	Small but distinct terrace. It is located in the mouth of the valley and it might be the proximal parts of a fan, deposited above sea level. It is too high compared with Eidesmoen.
37	Eidesmoen, E of Evanger	60.639	6.2083	66.3	66.2	67.2		10900	Large ice-marginal terrace, some 200 × 200 m and several lower, erosional terraces.
38	Dyrve, Voss	60.6282	6.309	70.5	79.0	82.0		11020	Here is a step in the slope that we consider to be a shoreline, some 300 m long and 30 m wide.
39	Vannjolo, Voss	60.6043	6.3652	72.6	80.0	84.0	80-89[S]	11010	A distal, slightly sloping terrace on a delta from a tributary river. 90 × 80 m in area.
40	Bordalen, Voss	60.6171	6.4247	76.4	94.0	96.0	97[S]	11100	At the mouth of Bordalen there is a 500 m long fan and delta system with a stair case of terraces. There are ice-marginal glacifluvial deposits up to 270 m a.s.l. and a large supra-marine fan with roof point 110 m a.s.l. (Skreden, 1967). A distinct terrace is sloping from 104 to 94 m a.s.l. along a 400 m long stretch. We consider the latter as the most probable marine limit, although there is another large terrace about 82 m a.s.l.
41	Nordheim, Eidslandet	60.7382	5.81	41.9		59.5	58,3[K] 59-60[A]	11070	Kolderup measured a terrace at Eide, on the other side of the river, which is now almost removed by the gravel pit. The terrace at Nordheim is ~300 × 200 m, and parts are almost horizontal. An end moraine ridge crosses the proximal part of the terrace. We use this terrace as the marine limit in Eidslandet.
42	Myster, Eidslandet	60.7364	5.82	42.5	59.2	60.6		11060	Around Myster there are several small terraces with altitudes 59–60 m a.s.l., supporting the marine limit given at Nordheim. In the eastern end of the settlement (60.7355 N, 5.826 E) is a terrace up to 66.5 m a.s.l., but we consider this as a fan build above sea level.
43	Eikemo	60.7107	5.541	27.8	67.0	68.0	70,2[K] 68-70[A]	11400	Here is a large terrace 500 × 300 m, slightly sloping. The floor of river channels in the distal part are 67–68 m a.s.l.
44	Store Urdal	60.7058	5.563	28.8	62.0	63.0	65,8[K]	11300	In the valley is a long terrace tilting from 68 to 62 m a.s.l. Small and more distal terrace remnants are about 61 m a.s.l.
45	Stølen, near Nøttveit	60.754	5.687	35.5	52.0	54.0	53,8[K]	11050	We assume this is the terrace that Kolderup (1908) called Nøttveit. The terrace is only 30–40 m wide, 200 m long and sloping towards the fjord. It is located close to a brook, but it might also have been partly formed by slided till.
46	Romarheim	60.7387	5.637	32.9	57.0	58.0	57,1[K] 57-60[A]	11160	At Nordli, Romarheim, there was originally a large terrace, but it is now almost completely removed by gravel exploitation. A cemetery, founded around AD 1900, is located on the only remnant flat part. Similar altitudes are found on other small terraces, whereas a sloping fan surface continues up-valley.
47	Granheim, Modalen	60.8277	5.848	43.6	50.0	51.0	53,6[K]	10900	Kolderup probably measured a terrace located near the sea and which is now removed by gravel exploitation. Granheim is located about 3 km up-valley and this deposit will probably be completely removed by 2018. The remnant terrace is 60 × 50 m, altitudes 51.0–50.0 m a.s.l. The gravel pit shows long foresets, >30 m high, in sand-gravel-cobbles. Topset is partly removed by bulldozers, but was apparently ~2 m thick. We consider the terrace represents the marine limit.
48	Helland, Modalen	60.8331	5.875	45.2	48.0	50.0		10860	This is one of the largest terraces in the area, c. 1 × 1 km. On the surface are distinct river channels, up to 5 m deep. The terrace is located below a high waterfall in the main river; the altitude of the river is 18.7 below and 55.6 m a.s.l. above the waterfall. We consider the terrace to represent the marine limit and that the ice margin was located shortly up-valley of the waterfall. The marine limit altitude is supported by the highest point, 50–52 m a.s.l., on a fan at Eikhaugane, 1.5 km down valley.
49	Andvik, northern end of Storevatnet	60.8109	5.385	18.6	52.8	53.8	57,4[K]	11350	Ice-marginal delta deposited in front of a glacier tongue in the lake Storevatnet. The measured flat surface is c 100 × 30 m and located east of the river outlet. Bedrock knobs in a closed gravel pit in proximal part shows that the gravel deposits were 10–30 m thick.
50	Totland, 1.5 km north of Andvik	60.8243	5.384	18.6	55.8	56.2		11400	Distinct terrace c 100 × 70 m, formed as a river delta and certainly showing the marine limit.
51	Solheim	60.8908	5.467	22.6	56.0	57.0	57[K]	11280	Here is a mall terrace at the river mouth, the flat surface is only some 20 × 20 m, but sediment cover continues in this elevation. Appears as a clear marine limit.
52	Haugsvær	60.9021	5.517	26.3	60.0	61.0	60.1-60.5[K]	11380	Most of this terrace, including the entire distal part, is removed and the former gravel pit is overgrown with dense forest. We measured a flat surface in the western part. Most of the rim of the former gravel pit is 63–64 m a.s.l., but this is obviously the proximal part of the original terrace. Our altitude might suggest a slightly too high age.

(*continued on next page*)

Table 1 (*continued*)

Site no	Site	Lat. **N** EU89	Long. **E** EU89	Dist.[a] Km	Distal part of terrace. m a.s.l. From	To	Refs.[b]	Age[c]	Comments
	Haugsdal, Kjetland.	60.8317	5.527	32	61.3	65.3			Haugsdal is a narrow valley with a train of terraces. The highest and most up-valley terraces are found on both sides of the river at Kjetland. However, they have so steep down-valley slope that we consider they were formed above sea level.
	Haugsdal, Storemyr	60.8332	5.513	31.3	58.3	58.7			At Storemyr, located about 0.8 km down-valley from Kjetland, is a distinct and flat terrace, 100 × 200 m in area that possibly represents the marine limit.
	Haugsdal, Vangen	60.8411	5.515	31.3	57.4	57.7			About 2 km down-valley from Kjetland is a closed gravel pit in a terrace showing steep foresets in sand and gravel covered by a less than 1 m thick topset. This clearly shows a marine level, probably the marine limit.
53	Haugsdal, conclusion	60.8411	5.515	25.4	57.4	58.7	60[K]	11300	It is difficult to determine the marine limit in Haugsdalen; we use the elevation span from Vangen to Storemyr.
54	Matre, west of the river	60.8772	5.581	29.3	60.5	61.5	61.3-63.5[K]	11280	The largest terrace was originally on the east side of the river, but it has been entirely removed by the gravel pit. Kolderup (1908) measured the flat part here to 61.3 m a.s.l. The terrace on the west side is well preserved and can be mapped over a distance of c. 300 m with altitudes from 66 m a.s.l. at the root point to a flat distal part 60.5–61.5 m a.s.l.
55	Store Sleire	60.8888	5.223	10	45.0	45.5		11380	Distinct delta where the river Myrdalselva ended in the sea. About 150 m across.
56	Skogaselshagen, Strandebarm	60.2800	5.9982	46.4	90.0	91.0	91-94[H]	11420	A distinct terrace some 200 m long, but only 15–20 m wide, is seen along Strandadalen. Co-ordinates given for southern end. We consider it to represent marine limit.
57	Botnen	60.4811	6.209	62.5	86.0		90–94[H]	11170	LiDAR covers only part of the valley, but we assume a 200 m long, flat terrace represents the marine limit. Hamborg (1983) gives considerably higher values, which would give correspondingly earlier deglaciation.
58	Haugen, Granvin	60.5799	6.675	89	97.0		95–96[H]	11000	According to Mæland (1963) this is the highest terrace in this valley. It is located freely in the valley and is obviously an ice-marginal delta.
59	Ulvik	60.5709	6.9098	102	123.0		120[H]	11160	Using an earlier version of the diagram, and the elevation 125 m a.s.l., Mangerud et al. (2013) gave an age of 11,100 for this terrace.
60	Eidfjord	60.4602	7.0864	110	104.0		102-113[H]	10940	Using an earlier version of the diagram and 102 m a.s.l., Mangerud et al. (2013) gave an age of 10,900 for this terrace.

[a] Distance from the 40 m Younger Dryas isobase.
[b] The highest terrace according to previous publications: K - Kolderup (1908); A - Aa and Mangerud (1981); H - Hamborg (1983); S - Skreden (1967).
[c] Age is calculated from the mean of the two given altitudes.

of the underlying topography, and directed approximately towards west in the entire area during periods when the highest mountains were covered by thick ice (Fig. 10A), as was also found by Hamborg and Mangerud (1981) and Aa and Mangerud (1981).

4.3.3. *Reconstruction of the ice sheet at 14,000 and 13,000 BP (Fig. 10B)*

A number of radiocarbon dates show that the coast was deglaciated about 14,800 BP, and the ice margin continued to retreat until about 13,000 BP. Sites where mollusc fragments incorporated in till have been radiocarbon-dated show the minimum inland retreat before the YD re-advance (Mangerud et al., 2016). The ice margins for the time slices 14,000 and 13,000 BP in Fig. 10B are taken from Mangerud et al. (2017). We discuss some of the dynamics of ice retreat from the outer coast in section 5.4. However, inside the YD ice margin it is impossible to securely identify striae that relate to ice flow from these periods, although some probably survived the YD re-advance.

4.3.4. *Reconstruction of the ice sheet during the Younger Dryas (YD), 11,600 BP (Fig. 10B)*

During the YD there was a major glacial re-advance across most of the studied area (Mangerud et al., 2016) (Fig. 10B). In some places, glacial ice more than 1.5 km thick refilled fjords that were ice-free during the foregoing Allerød interstadial. The Herdla Moraine, mapped after field investigations across the entire study area by Aarseth and Mangerud (1974), marks the outermost YD ice margin in the study area. We use this line with a few minor modifications based on examination of aerial photos (Sæle, 2017) and LiDAR-derived DTMs, as the maximum extent of the YD ice margin (Fig. 10B).

Near the end of the YD there was a sea-level highstand that

Table 2
Sources for the glacial striae.

No of striae	Reference
1410	J. Mangerud, unpublished field notebooks 1963–1966 and 2016–2018
36	Mæland (1963)
138	Skreden (1967)
202	Aarseth (1971)
454	Aa (1974)
34	Aarseth and Mangerud (1974)
243	Hamborg (1979)
288	Skår (1975)
49	Olsen (1977)
48	Sæle (2017)
2903	Total number

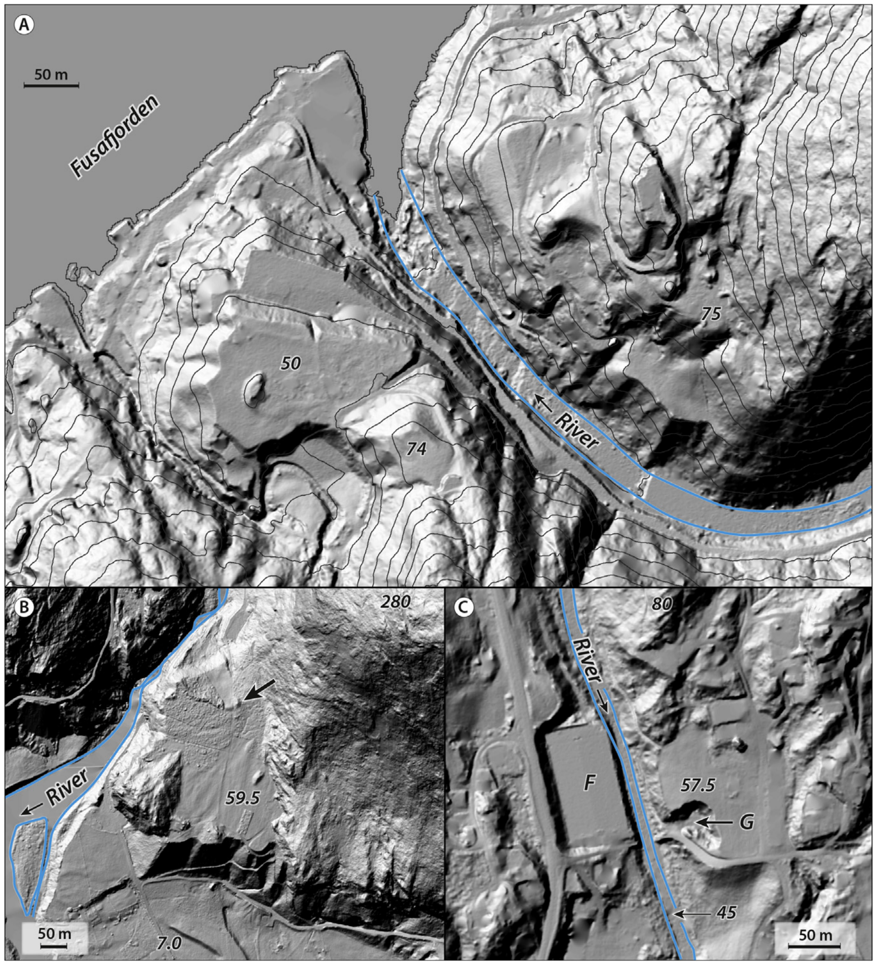

Fig. 6. Hill-shaded renditions of 2 m resolution Digital Terrain Model to show typical morphology of selected marine limit terraces. Numbers show altitudes in m a.s.l.
A. Marine limit terraces at Tysse (No. 8 in Table 1, Fig. 9) marked with elevations, 75 at the NW side and 74 a.s.l. at the SE side respectively (see Fig. 7A). Contour interval is 10 m.
B. The marine limit terrace at Nordheim, Eidslandet (No. 41). Arrow shows the small moraine at the proximal end. Note the river channels besides the altitude mark for the marine limit, 59.5 m a.s.l.
C. Marine-limit terrace (57.5 m a.s.l.) at Søfteland (No. 11). This terrace originally filled the valley but has been modified. G = closed gravel pit. F = football pitch on site of former gravel pit excavated into the same terrace.

lasted for 240 years and probably ended some decades into the Holocene (Lohne et al., 2004, 2007). The 240-years long duration of the highstand does not cause any uncertainty in the dating of the younger terraces as the age of these are related to the very end of the highstand, which is well dated to 11,550 BP (Fig. S1) (Lohne et al., 2007). However, Lohne et al. (2004) have shown that ice-margin retreat started 50–100 years before the end of the sea-level highstand and the start of retreat is also independently dated to 11,600 BP (Lohne et al., 2012). Accordingly, in this study we use 11,600 BP as the age for ice-margin retreat from the Herdla Moraine and 11,550 BP for the onset of fast sea-level emergence.

A dense net of measured striae along the Herdla Moraine show that ice-flow directions close to this margin were mostly perpendicular to the margin. To extend the ice-flow paths inland we correlate striae near the margin with “next-youngest” striae up-flow, because the very youngest striae commonly were formed during the final retreat. We also use striae on low mountain plateaus that were covered by YD ice, based on mapped ice-surface slopes along Fanafjorden, Fusafjorden, and Hardangerfjorden, and which became ice-free as soon as the ice surface was slightly lowered.

Striae clearly show that ice flowed out of Hardangerfjorden, across low mountains (up to 700 m a.s.l.) towards a calving, and probably floating, ice margin in Bjørnafjorden (Bondevik and Mangerud, 2002) (Fig. 15). Fusafjorden, a tributary fjord to Bjørnafjorden, drew ice from the mountains to the northeast, which alternatively would have drained towards the larger Hardangerfjorden. High mountains (600–900 m a.s.l.) along the western side of Fusafjorden forced the YD ice to follow the fjord and flow towards SW.

In contrast to the concentrated flow following Fusafjorden, northwards towards Fensfjorden, ice spread out like a fan, forming a surprisingly even ice front considering the complex underlying topography (Fig. 10B). In the southern part high mountains influenced the pattern of the margin, but along Hjeltefjorden it was apparently a straight and floating margin. We have fewer observations of striae in the northern area, but it is remarkable that the ice apparently flowed obliquely across all the fjords, including the up to 700 m deep Fensfjorden to produce the S–N oriented moraine. Since the YD ice margin represents the configuration of an advancing ice sheet, one may almost ask if a thick, advancing ice sheet is less prone to follow the topography, or to form ice streams, than stable or retreating ice margins.

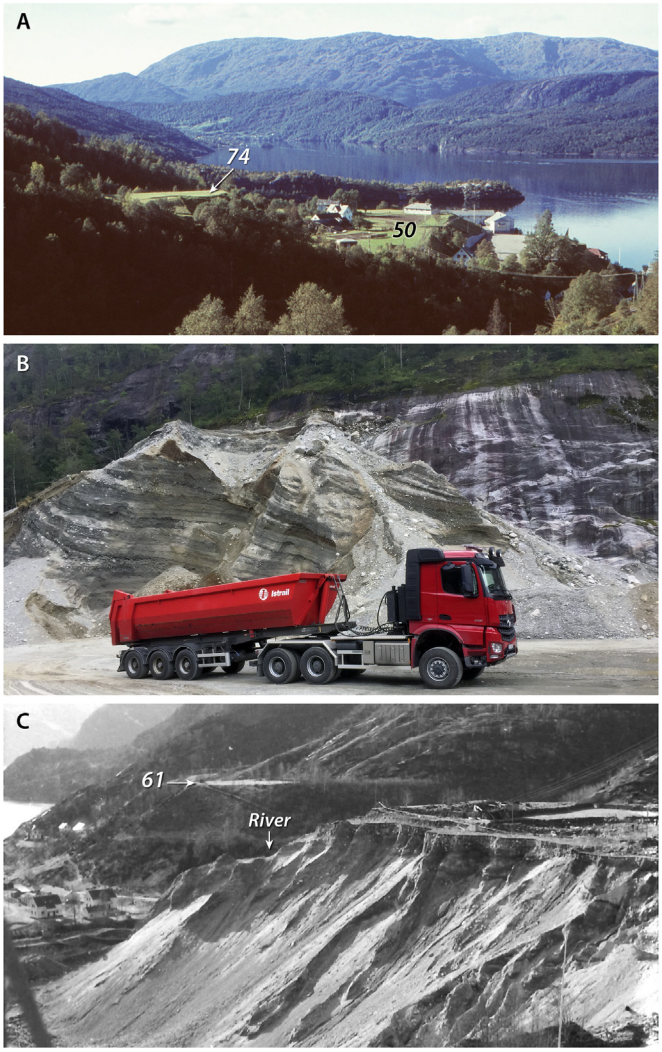

Fig. 7. Photos of marine limit terraces.
A. The terraces south-west of the river in Tysse, Samnanger (No. 8, Table 1). The arrow points to the 74 m a.s.l. terrace, located 1 m lower than the marine limit terrace in the opposite side of the river (Fig. 6A). The photo is taken across the river, towards west; the mountain to the right in the background is Gullfjellet in Bergen (990 m a.s.l.). Photo JM, 1975.
B. Granheim in Modalen (No. 47, Table 1). This is a typical section in ice-front deltas in the study area, with long foresets consisting of coarse sand and gravel, here about 35 m high. The topsets have been removed. A small remnant of the marine limit terrace was still left on the top (not seen), but will soon be removed. Photo JM, 2017.
C. The marine limit terraces in Matre (No. 54, Table 1). The terrace in the foreground (i.e. east of the river) is now completely removed by gravel excavations. We measured the marine-limit terrace on the west side of the river (marked 61 m a.s.l.). The fjord is seen in the background. Photo JM, 1963.

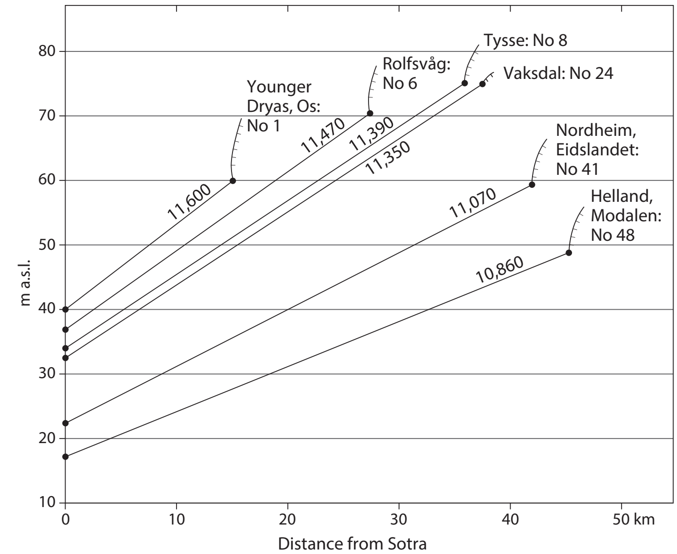

Fig. 8. Dating ice-margin positions with the shoreline diagram. Selected ice-marginal deltas are plotted in the Master shoreline diagram. Decadal ages are interpolated between the lines shown on the Master diagram (Fig. 5). Note that real distances of ice-margin retreat are considerably longer than shown in the horizontal scale here, for example from Os to Helland is more than 80 km. This is because distances in the diagram are measured at right angles to the isobases, whereas ice retreat was partly parallel with the isobases. The 11,550 and 10,860 are the oldest and youngest shorelines used in our study, respectively.

4.3.5. *Reconstruction of the ice sheet at 11,500 BP (Fig. 11A)*

At this time the Os Valley (Fig. 15) became a shallow marine inlet along Bjørnafjorden, with a maximum depth of about 58 m (the elevation of the marine limit), except where lakes are presently located. At the end of the YD, the ice margin calved in Bjørnafjorden but also formed a lobe into the lake Ulvenvatn (Fig. 15) where it deposited a marine ice-marginal delta (Bondevik and Mangerud, 2002). During the first 160 years of retreat, three more ice-marginal deltas were deposited up-valley, and which could be precisely dated with the shoreline diagram (Fig. 15B), allowing us to determine the rate of retreat at decadal resolution. Measured along the flow line, the ice-marginal terraces at Hetlefloten (no.10), dated to 11,530 BP, Søfteland (no. 11) 11,480 BP and Gåssand (no.12) 11,440 BP are located 4.5, 7.5 and 9.5 km from the YD margin at Ulven (11,600 BP) respectively, giving a mean retreat rate of about 60 ma^{-1}. During this short period, there was considerable re-organisation of the ice margin recorded by striations along the lake northeast of Hetlefloten (Fig. 15). The dense net of observations here is due to artificial lowering of the lake level, which caused clay-silt slides that exposed fresh striated bedrock (Fig. 3). The older striae show down-valley flow whereas the younger striae show flow towards the deeper part of the lake (which was part of the fjord during the deglaciation). This pattern reflects faster calving in the deeper part of the paleo-fjord. Thus, during retreat to the north the margin became oriented SW-NE and finally, almost S–N.

The reconstructed ice tongue in the Os Valley was isolated from the outlet glacier in Fusafjorden by high mountains. Most of the striae along Fusafjorden are parallel with the fjord, indicating a typical marine-terminating outlet glacier with a straight front across the fjord. The retreat rate of the ice front in Fusafjorden was about 160 m a^{-1} from 11,600 to 11,500 BP.

In the pass from Sørfjorden over to Fusafjorden, there is a large number of striae that show persistent southerly ice-flow from Sørfjorden to Fusafjorden (Fig. 4 and Fig. S1). The pass is about 260 m a.s.l., but striae directed towards the south are found up to 890 m a.s.l. We consider that this flow started about 11,500 BP, because the fast retreat in Fusafjorden would have increased the ice surface gradient towards the south, drawing ice flow in that direction. This flow must have cut off ice flow from the ice sheet to the mountain Gullfjellet (marked G in Fig. 11A).

Two large ice-margin deltas (Fana and Stend, Fig. 14), which plot on the 11,550 BP shoreline, are located at the head of Fanafjorden, about four km inside the Herdla Moraine that is crossing the fjord mouth (Fig. 14). The simplest interpretation is that the ice margin retreated from the Herdla Moraine 11,600 BP and stabilized at the Fana and Stend ice-front deltas soon after the YD/Holocene transition and thus before the sea-level started to drop from its highstand position. In the area north of Fanafjorden the ice retreat is for

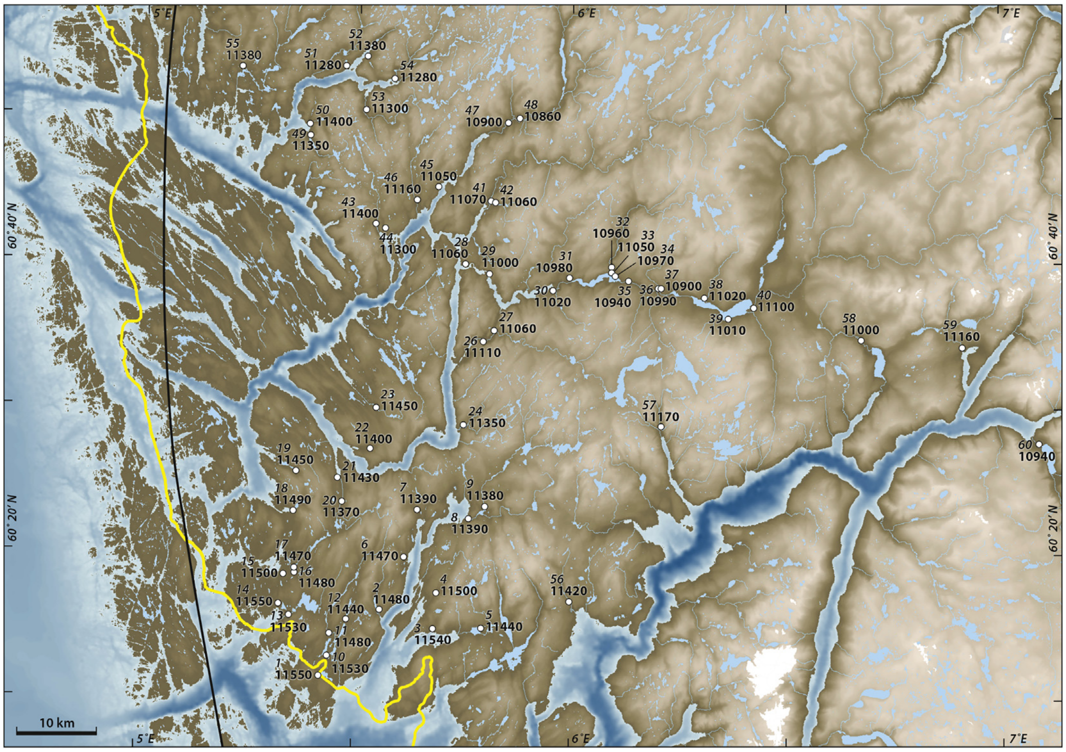

Fig. 9. Location and age of ice-marginal deltas and other Marine Limit terraces. The small numbers refer to the terrace number in Table 1. The yellow line shows the Herdla Moraine of YD age. The black line shows the YD 40-m isobase. (For interpretation of the references to colour in this figure legend, the reader is referred to the Web version of this article.)

Fig. 10. Reconstructed ice-flow patterns.
A. Periods when the ice sheet was thick, for example 15,000 BP.
B. Younger Dryas (YD) ice margin and flow lines. Thin yellow lines show the approximate ice margin positions at 14,000 and 13,000 BP (Mangerud et al., 2017). (For interpretation of the references to colour in this figure legend, the reader is referred to the Web version of this article.)

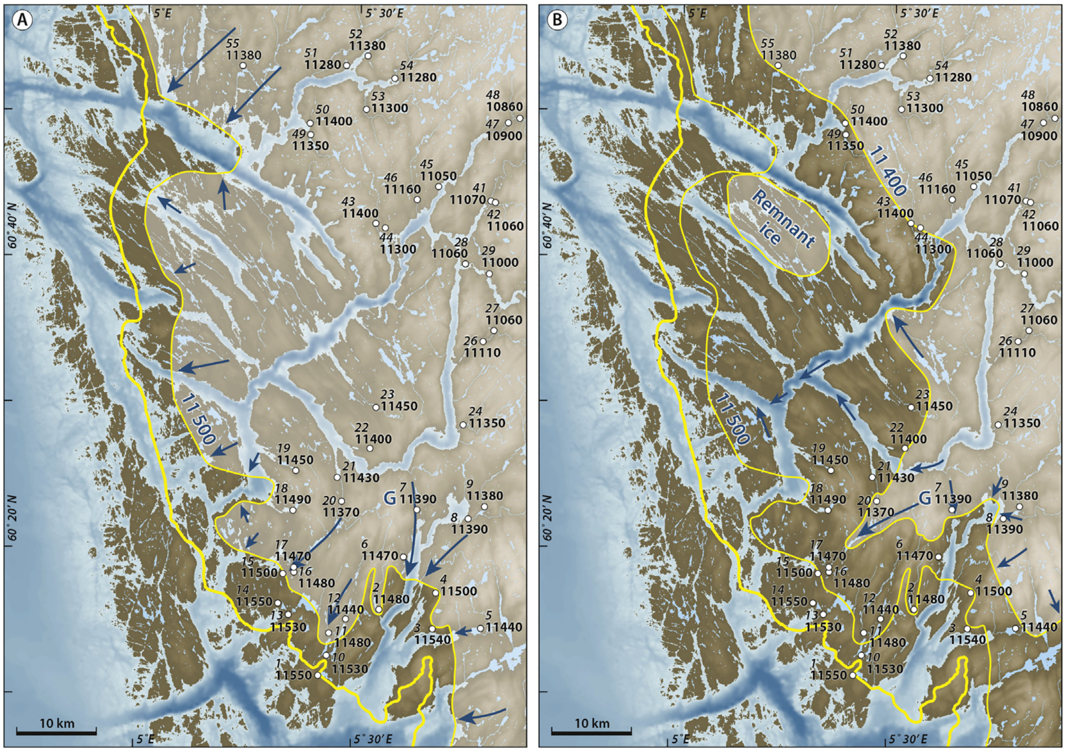

Fig. 11. Reconstructed ice margins and flow lines.
A. 11,500 BP. The Herdla Moraine is kept on the map in order to see the retreat pattern. G – Gullfjellet.
B. 11,400 BP. Some flow directions for the period between 11,500 and 11,400 BP are marked. The older ice-margin lines are kept on the map in order to see the retreat pattern.

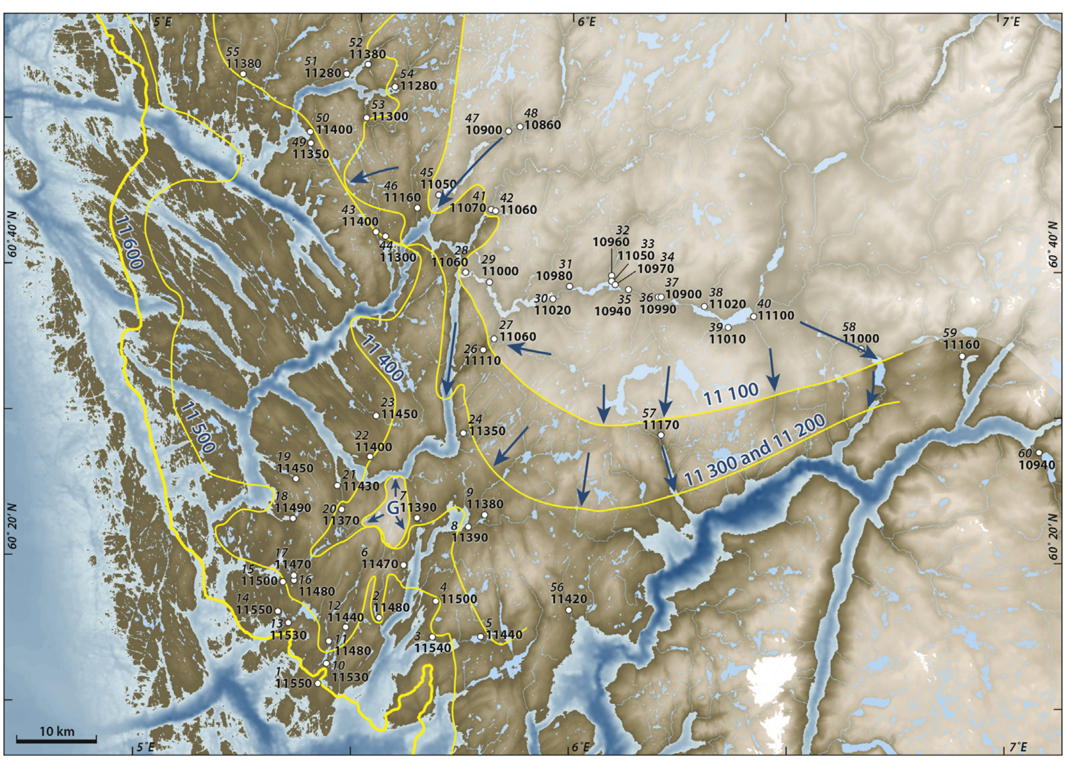

Fig. 12. Reconstructed ice margins and flow lines. 11,300 BP to 11,200 and 11,100 BP. Older ice-margin lines are kept on the map in order to see the retreat pattern.

five km dated at a decadal resolution using the ice-front deltas at Stend (no.14, 11,550 BP), Skjold (no.15, 11,500 BP) and Elveneset (no.16, 11,480 BP) (Fig. 14A). Further north, the ice in Byfjorden had retreated to the site of the present-day city of Bergen (no. 18,

Fig. 13. The 11,000 and 10,900 BP ice margins. We have not considered the amount of ice in the eastern area at 11,000 BP, but marked the Eidfjord-Osa Moraine (Anundsen and Simonsen, 1967; Vorren and Mangerud, 2008) dated to 10,900 BP (Mangerud et al., 2013).

Årstad) at 11,490 BP, as described in section 5.4.

We have not been able to identify terraces dated to about 11,500 BP in the entire area north of Byfjorden and therefore we tentatively extend the ice margin northwards by drawing a line at right angles to the youngest striae. The reconstruction of the ice margin is much more uncertain here than further south.

4.3.6. Reconstruction of the ice sheet at 11,400 BP (Fig. 11B)

Between 11,500 and 11,400 BP there was major retreat and reorganisation of the ice margin. Still, the changing flow directions and pattern of the ice-margin retreat can be reconstructed in great detail along some of the fjords.

We describe the retreat by iceberg calving in Byfjorden in section 5.4. Further up fjord, near the junction of Byfjorden and Herdlafjorden, the youngest striae along Herdlafjorden show a calving bay with ice flow from the SE, suggesting that Herdlafjorden became ice-free before Byfjorden (and Askøy) (Fig. 11B and Fig. S1). This interpretation is supported by the pattern of striae at the junction of the two fjords, which shows that ice flow from the north turns into Herdlafjorden but not into Byfjorden suggesting that thicker ice remained in Byfjorden and deflected the ice flow. Between here and the calving bay in the southern end of Byfjorden (section 4.3.5) almost all striae show ice flow across the fjord, suggesting a retreating ice front parallel with the fjord orientation. An explanation might be that the two ends of the fjord became ice-free almost contemporaneously and thus the fjord between them broke up very fast.

We have fewer observations near the next fjord junction to the NE, but striae on Osterøy suggest that the last flow direction was from Osterfjorden (Fig. 11B). This interpretation is consistent with the general picture of ice retreat towards the NE. In Sørfjorden, i.e. SSE from the mentioned fjord junction, the last ice flow generally followed the fjord towards the NNW. The pattern is much more complicated in the tributary inlet and valley to the south of Sørfjorden (terraces Indre Arna, no 20 and Mjeldheim, no 21, Fig. 11B). Here the oldest ice flow was towards the west, thus obliquely across the valley, as also shown by striae on the bordering mountains. A younger set of glacial striae shows ice flow towards the south, i.e. up valley, which according to our reconstruction took place sometime between 11,500 and 11,400 BP, when the ice surface was lower than the valley walls and the ice margin was still located to the south. The final ice flow was in the opposite direction, towards the north, indicating that the ice had retreated in Sørfjorden to allow normal down valley ice flow. There is an apparent conflict between the altitudes and concluded ages of the terraces in this valley. Mjeldheim (no. 21) and Indre Arna (no. 20) are located close to each other yet Mjeldheim yielded an age 60 years older. The explanation might be that the terrace at Mjeldheim was deposited by a river from the west when the mouth of the valley became ice-free, whereas the terrace at Indre Arna was formed by meltwater from a valley glacier from Gullfjellet that survived some few decades longer.

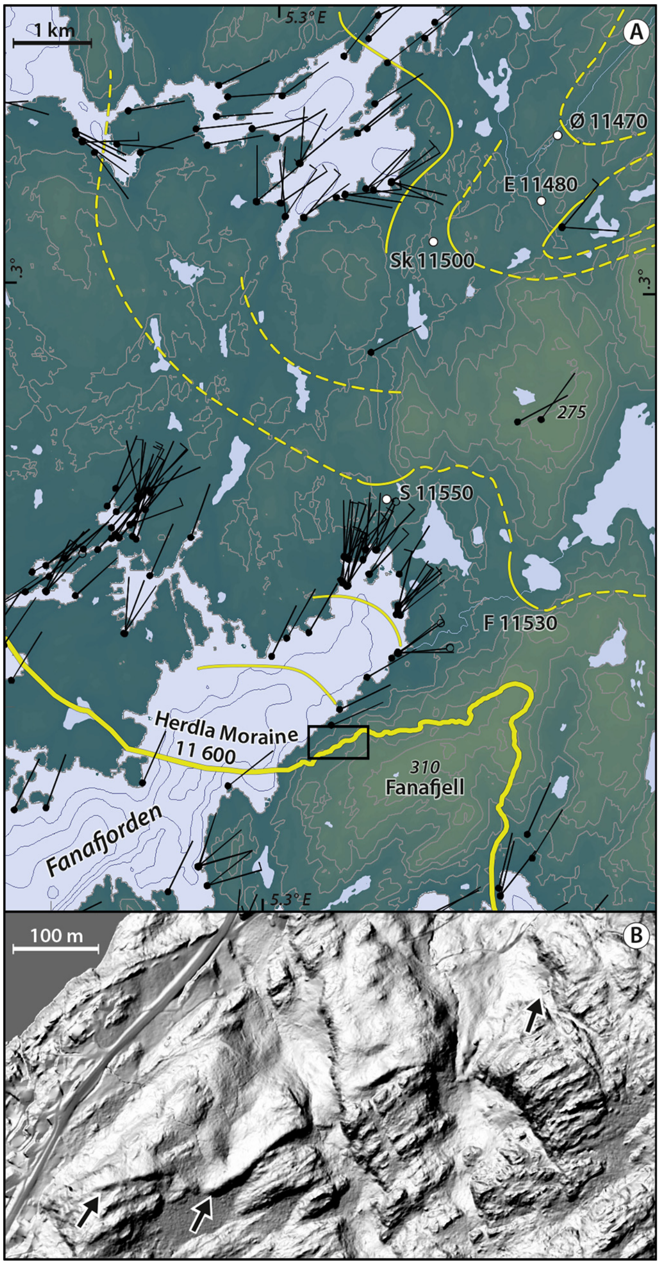

Fig. 14. Deglaciation of the Fana area.
A. Map with striae, deglaciation pattern (yellow dashed/full lines) and age on terraces (F – Fana, No. 13; S – Stend, No. 14; S – Skjold, No. 15; E – Elveneset, No. 16; Ø – Øvsttun, No. 17). For location see Fig. 2.
B. LiDAR image of the lateral moraine on Fanafjell (box in A), marked with arrows. Note that there is a thin (<1m) till cover proximal and only exposed bedrock distal to the moraine. (For interpretation of the references to colour in this figure legend, the reader is referred to the Web version of this article.)

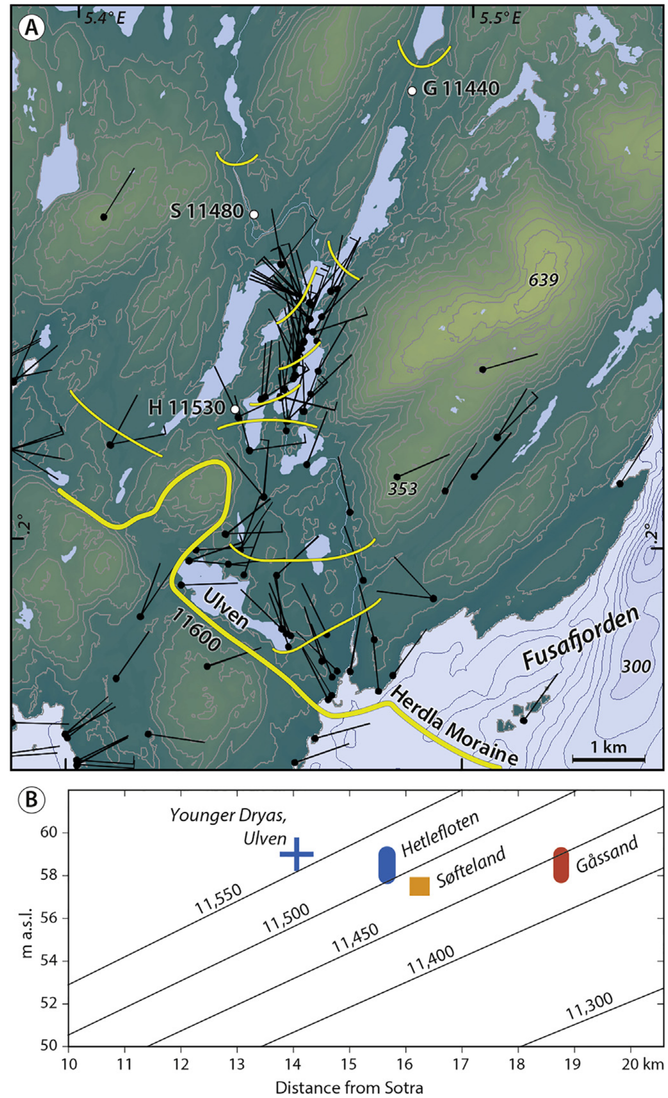

Fig. 15. Glacial geology and chronology of the Os Valley.
A. Glacial geological map; for location see Fig. 2. Ice-front deltas are marked with letter and age: H – Hetlefloten (No. 10, Table 1); S – Søfteland (No. 11), G – Gåssand (No. 12). Some ice margins, mainly based on glacial striae orientations, are marked with yellow lines. Contour interval 50 m; some altitudes on land and depths in the fjord are given with numbers. Legend for striae, see Fig. 4.
B. Enlarged part of the Master Shoreline Diagram (Fig. 5) with the terraces (the altitude range) in the Os Valley plotted (Table 1). Note that all have approximately the same altitude, but due to the tilted uplift, their ages are different. (For interpretation of the references to colour in this figure legend, the reader is referred to the Web version of this article.)

The glacial striae at higher elevations on Osterøy show ice flow towards W or SW across the island, whereas the youngest striae found along the lake Vestrevatnet record a flow direction towards NW, i.e. reflecting a switch of up to 90° (Fig. 16). According to our reconstruction, Osterfjorden became ice-free before Sørfjorden-Veafjorden. We postulate that when the outlet glacier in Osterfjorden broke up, ice from the areas adjacent to the fjord started to flow towards the fjord, and that this north-westerly flow direction propagated up flow to include relatively thick ice on Osterøy.

Striations along the shores of Veafjorden indicate that the youngest ice flow here was directed due south (Fig. 16). We infer that this southerly ice flow started when the ice surface was low enough for the fjord topography to control ice flow and must post-date northwesterly ice flow on Osterøy.

We have fewer observations of both terraces and glacial striae in the northern part of our study area. However, Fensfjorden likely became ice free at or around the same time as Osterfjorden. Striae on the shores of Fensfjorden show flow towards the fjord, suggesting that ice remained on both the low Lindås Peninsula to the SW and in the mountains to the NE, after deglaciation of the fjords (Fig. 11B). Glaciers from mountain plateaus to the NE of Fensfjorden reached the middle part of the tributary fjords by 11,400 BP and we assume an ice cap covered the plateau at this time.

In the southern part of our study area, the ice margin had

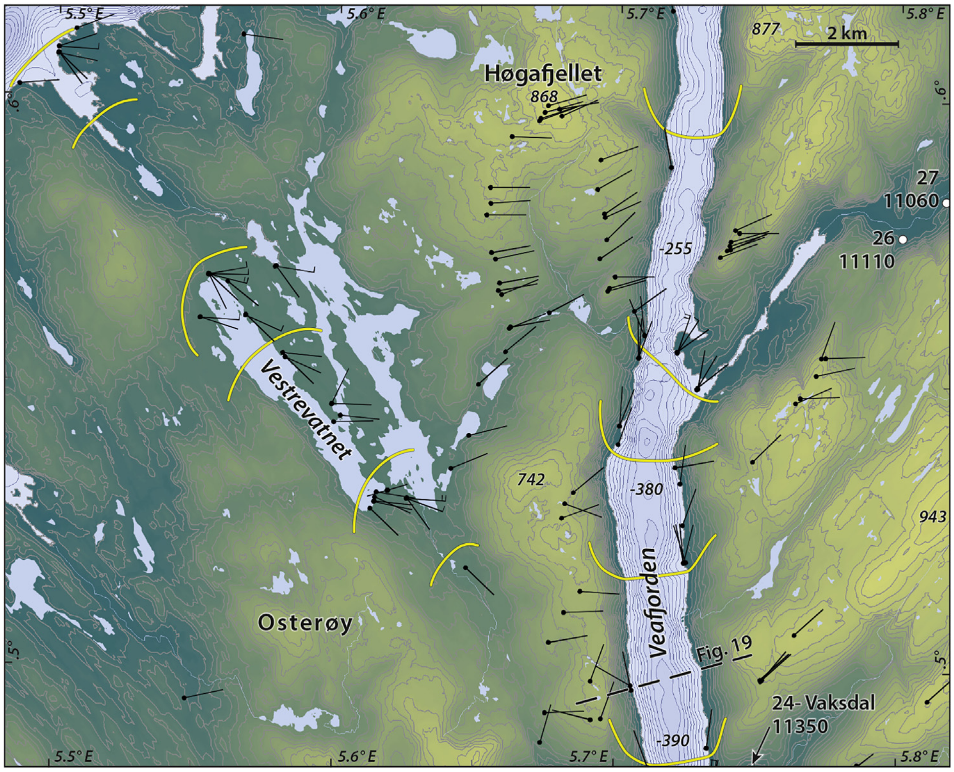

Fig. 16. Glacial striae on Osterøy and along Veafjorden. Terraces are marked with number: No. 24 – Vaksdal; no. 26 – Dalegården, Dale; no. 27 – Dale. Some arbitrarily spaced ice-margins, based on flow directions, are shown with yellow lines. Some mountain altitudes (m.a.s.l.) and fjord depths (m) are marked. Dotted line shows the profile shown in Fig. 19. (For interpretation of the references to colour in this figure legend, the reader is referred to the Web version of this article.)

retreated to the head of Fusafjorden where striations show ice flow converging towards the fjord. The surface of the ice flowing from Sørfjorden to Fusafjorden, mentioned in section 4.3.5, likely also lowered creating conditions for the isolation of a remnant ice cap over Gullfjellet, described in the next section.

4.3.7. Reconstruction of the 11,300 and 11,200 BP ice sheets (Fig. 12)

We have no observations that allow us to differentiate the 11,300 and 11,200 BP ice margin positions. The terraces in both Veafjorden and Osterfjorden suggest that the ice margin position remained stable during this period. Therefore, we draw a single line on the map for both 11,300 and 11,200 BP (Fig. 12).

The most striking differences from 11,400 BP are a major retreat in Hardangerfjorden and in Sørfjorden-Veafjorden to the north of Vaksdal (terrace no. 24, Fig. 12), indicating that the southerly-directed striae along the shores of Veafjorden (Fig. 16) were formed during the period 11,300 to 11,200 BP. In the absence of information on ice flow directions feeding this fjord glacier, we assume that west of Veafjorden it was bounded by the fjord wall, whereas it was connected to, and received ice from, the eastern side of this fjord. In Osterfjorden, further north, the ice margin remained stable between 11,400 and 11,200, whereas near Masfjorden the ice margin had retreated to the head of the fjord.

The youngest glacial striae, although only two, along Sørfjorden show ice flow from an ice mass over Gullfjellet that must have remained after ice in the fjord had broken up, i.e. after 11,400 BP (Fig. 12). The pattern of striae suggests that this ice mass had considerable extent as the youngest striae around the mountain plateau show radial ice flow, especially down the valleys. We do not find any ice marginal deposits around the mountain, nor do we have information on the final date of deglaciation of this mountain, but probably the dome melted away sometime between 11,400 and 11,300 BP. We discuss some climatological implications of this ice cap in section 5.1.

4.3.8. Reconstruction of the ice sheet at 11,100 BP (Fig. 12)

The 11,100 BP ice margin was also located close to the 11,300 (and 11,200) BP margin positions, most notably in the Veafjorden-Osterfjorden area. We have there drawn a small retreat, but the difference is almost within the dating precision. The 11,100-margin is supported by a basal lacustrine radiocarbon date close to terrace no. 28 that yielded an age of 10,600–11,800 cal BP at the 95.4 significance interval (Aa and Mangerud, 1981). Further to the north, the ice margin now terminated on land, such that no marine terraces were formed and we have therefore no further dating information.

Most important for the overall pattern of retreat is that ice in Hardangerfjorden had broken up all the way into Ulvik (terrace no. 59, Fig. 12) by this time, and that the ice margin had retreated to the north of the terrace at Botnen (no. 57, Fig. 12). This led to a switch in ice flow southwards and towards Hardangerfjorden across the entire area and we infer that the ice sheet thinned northwards following thinning and break-up of the Hardangerfjorden outlet glacier. This switch in ice flow direction towards Hardangerfjorden is recorded by numerous glacial striae, including SE-directed striae in the valley between Voss and Granvin (no. 58), where the watershed is located at only 250 m a.s.l.

4.3.9. Reconstruction of the ice sheet at 11,000 BP (Fig. 13)

All 13 terraces along the 40 km-long valley from Veafjorden to Voss give ages between 10,940 and 11,100 BP, suggesting that deglaciation took place between 11,100 and 11,000, and probably rapidly in the first part of that century. Taken at face value the oldest of the obtained ages are for the terraces in the eastern end of the valley. However, considering that most of the terrace remnants along this valley are small, the age differences are probably within measurement error.

Glacial striae show that the youngest recorded ice flow was directed westwards down-valley, and there are some small ice-margin deposits suggesting up-valley ice retreat, indicating a second 90-degree switch in ice flow from the preceding and successive stages. Most of the valley is narrow and likely formed a shallow fjord branch during deglaciation. Even though the sea penetrated all the way to Voss, it was not deep nor wide enough to favour fast calving and retreat. We conclude that the fast deglaciation was facilitated by earlier strong thinning along the entire valley due to drawdown towards Hardangerfjorden, as described in section 4.3.8.

4.3.10. Reconstruction of the ice sheet at 10,900 BP (Fig. 13)

The youngest ice-marginal terrace we have identified is located at Helland in Modalen (no. 48), dated to 10,860 BP (Fig. 13). The large dimension of this terrace suggests that the ice margin halted for a period. This is supported by large ice-marginal deposits shortly up-valley, between the terrace and a lake to the north (Olsen, 1977). The terrace itself is located just below a 35 m-high waterfall and does not have any morphological ice-contact slope. According to our shoreline diagram, the Helland Terrace is of the same age as the Eidfjord-Osa Moraine near the head of Hardangerfjorden, which outlines a long outlet glacier extending to Voss (Fig. 13) (Anundsen and Simonsen, 1967; Mangerud et al., 2013). The prominent Eidfjord-Osa Moraine has been mapped for long stretches and the pattern indicates that it represents a re-advance indicative of a decline in summer temperature and/or increased winter precipitation. If the Helland Terrace is indeed contemporaneous, then there must have been an isolated ice cap in the mountains north of Helland that was separated from the ice sheet forming the Eidfjord-Osa Moraine (Fig. 13).

4.3.11. The final disappearance of the ice

Our chronology is based on ages of marine terraces derived from our shoreline diagram, which restricts the application to areas below the marine limit. To our knowledge there are no radiocarbon ages constraining the timing of final deglaciation in the surrounding mountains that were still covered by ice at 10,900 BP (Hughes et al., 2016). However, no moraine systems are found in these mountains, probably suggesting that the ice melted down continually and quickly after 10,900 BP.

5. Discussions

5.1. Mass balance and the equilibrium line altitude (ELA)

The major re-advance of the southwest Scandinavian Ice Sheet during the YD reflects a lowering of the ELA relative to its height during the preceding Bølling-Allerød period, probably mainly caused by cooler and shorter summers. We infer that the ice sheet mass balance was at, or close to, equilibrium when the margin stabilized at the Herdla Moraine, when the ELA was 460–600 m-lower than present (Mangerud et al., 2016). With the warming at the YD/Holocene transition, the ELA started to ascend, and the rate of the rise in the ELA position is decisive for the rates of ice sheet thinning and ice margin retreat during the subsequent deglaciation.

Small patches of snow or ice have survived most summers during the last few decades in north-facing depressions on the mountain plateau Gullfjellet (Fig. 2), suggesting that the present-day ELA is near the summit altitude (990 m a.s.l.) (Mangerud, 1986). We have not found any moraine deposits, or other evidence, showing that an active glacier existed on the plateau after the main ice sheet melted away. Combined with our chronology of the ice marginal retreat from marine terraces, this suggests that the regional ELA had risen to an elevation close to the present-day ELA about 300 years after the onset of retreat at 10,600 BP. This conclusion is apparently in conflict with the fact that some young glacial striae show radial ice flow from the plateau (section 4.3.7), suggesting that an ice mass survived on Gullfjellet later than the ice surrounding the mountain. Our interpretation is that this ice mass was a remnant caused by fast outlet-glacier retreat in the surrounding fjords, and that the mass balance during deglaciation never was in equilibrium.

The fact that the ELA was close to the present-day altitude of the summit of Gullfjellet around 10,300 BP, does not imply that the ELA rose above the entire ice sheet because the ice sheet surface further inland was still located well above the present-day mountains and ELA positions. However, it is possible that the ELA rose so fast from 10,600 to 10,300 BP that the ice margin did not retreat fast enough to keep the ice sheet mass balance in equilibrium. This changed during the Preboreal Oscillation at about 10,300–10,100 BP, when the ice margin halted or retreated very slowly (section 5.6).

Fig. 17 shows the net balance relative to elevation for two present-day glaciers in western parts of Norway (Andreassen et al., 2005); Nigardsbreen (61.7 °N, 7.1 °E) located shortly north of Sognefjorden (Fig. 2) and Engabreen (66.7 °N, 13.8 °E) located along the coast of northern Norway, some 800 km north of our area with correspondingly colder climate. Both glaciers are outlet glaciers from large ice caps. Although theses curves are not directly applicable to the deglaciation period in western Norway, the climate during the Early Holocene was similar to present-day (Eldevik et al., 2014). The curves provide a rough estimate of potential melting rates, especially for isolated ice remnants to which flow from the main ice sheet had been cut off (section 5.4). If we use a melting rate of 10 m a^{-1} (Fig. 17), a 300-m-thick ice would melt away in 30 years, suggesting that ice masses that was dynamically cut off from the ice-sheet accumulation areas would melt away within some

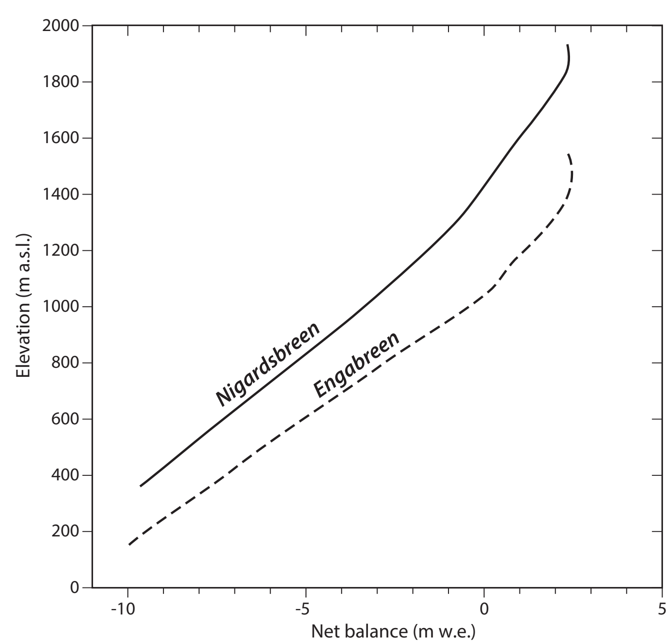

Fig. 17. Mean net balance versus altitude for Nigardsbreen and Engabreen for the period 1989–2003. Modified from Andreassen et al. (2005). M w.e. = meter water equivalents.

few decades.

5.2. Ice flow across deep fjords that are oriented perpendicular to ice-flow directions

We state above that the ice-flow directions were independent of the underlying topography when the ice sheet was thick, as ice flowed across several deep valleys and fjords. Still, deep fjords oriented N–S and thus perpendicular to the predominant ice flow direction challenge our curiosity. Did the basal ice flow down to the bottom and up again on the opposite side when ice-flow direction was at right angles to the fjord, or was the fjord bottom filled with dead ice or a subglacial lake (Fig. 19)? If the former, what stress-conditions did this create in the ice column? How and when were such fjords formed? We do not solve these fundamental questions, but instead provide some observations, and challenge other scientists to address these issues. To our knowledge, such observations or situations have rarely been discussed or modelled in the literature. Some early exceptions are from the Gudbrandsdalen area in eastern Norway (Bergersen and Garnes, 1972; Garnes, 1973; Garnes and Bergersen, 1977; Mangerud, 1965). In Vinstradalen glacial striae on the valley walls and fabric in basal till on the valley floor, show that ice flowed down to the bottom when crossing perpendicular to this valley (Fig. 19) (Mangerud, 1965).

The most spectacular of all the north-south-oriented fjords in our study area is Veafjorden (Figs. 16, 18 and 19), which is about 25 km long and only 0.7–1.4 km wide. The fjord has extremely steep walls from sea level all the way up to surrounding plateau summits at altitudes 600–900 m a.s.l. Considering that the water depth is more than 350 m in the entire southern half of the fjord, this means that the relative relief for this narrow fjord is up to 1300 m (Fig. 19). We have measured well-preserved striae, mainly on quartz lenses, on the mountain ridges along the fjord. On the western side of the fjord, we found numerous striae with directions around 260° from 180 m a.s.l. to the very summit at 870 m a.s.l. (Høgafjell) (Fig. 16). We searched along the shorelines of Veafjorden for striae with such directions, but only found striae oriented parallel with the fjord; if there had been striae with other directions they were subsequently erased. This is a reasonable inference, because as soon as the ice surface was located below the bordering mountains, the ice was forced to flow along the fjord and, as shown in section 4.3.2, such an outlet glacier flowed along Veafjorden for more than a century. In a recent model simulation described by Åkesson et al. (2018), the ice flowed across both Veafjorden and the fjords mentioned below. However, since the model did not include vertical shear, it could not resolve if or how the basal ice flowed across the fjord.

Raunefjorden, located east of Sotra (Fig. 2), is up to 250 m deep and mountains along the western shore of the fjord are up to 340 m high, giving a total relief of about 600 m. Glacial striae observed from sea level to the mountain summit show ice-flow directed across the fjord (Fig. 4 and Fig. S1). The pattern is the same for Hjeltefjorden, the extension of Raunefjorden to the north. This fjord is 300 m deep, but here the islands to the west are generally less than 50 m high. Byfjorden (Fig. 2) is 350 m deep, with mountains some 400 and 200 m high on the eastern and western sides respectively. Here, again, the oldest glacial striae indicate ice flow across, rather than along, the fjord.

If ice flowed down to the bottom of these fjords when the flow direction was perpendicular to the fjord direction, then this flow has similarities with ice flow conditions in over-deepened lake and fjord troughs. Sognefjorden, for example, has a maximum depth of more than 1300 m but is less than 200 m deep at the fjord mouth, requiring ice to flow down and then up-hill by more than 1100 m. However, there are major geometrical differences; Sognefjorden is long compared to its depth, with a length/depth ratio in the order of 100:1, whereas for our most extreme example Veafjorden this ratio would be less than 3:1. In Sognefjorden ice would also have been laterally restricted by the adjacent mountainsides, whereas ice flowing across Veafjorden had no lateral topographic boundaries at this time.

We assume that almost no erosion would take place in the deeper parts of the fjords during periods when the ice flowed across them, even if ice moved all the way to the bottom, because

Fig. 18. Air photo of Veafjorden. The photo is taken towards north. In the foreground one can see Sørfjorden that continues to the left (west). The village to the right is Vaksdal. The same mountain altitudes (m a.s.l.) and fjord depths as in Fig. 16 are marked. Photo: Geir Helge Johnsen, Rådgivende Biologer AS.

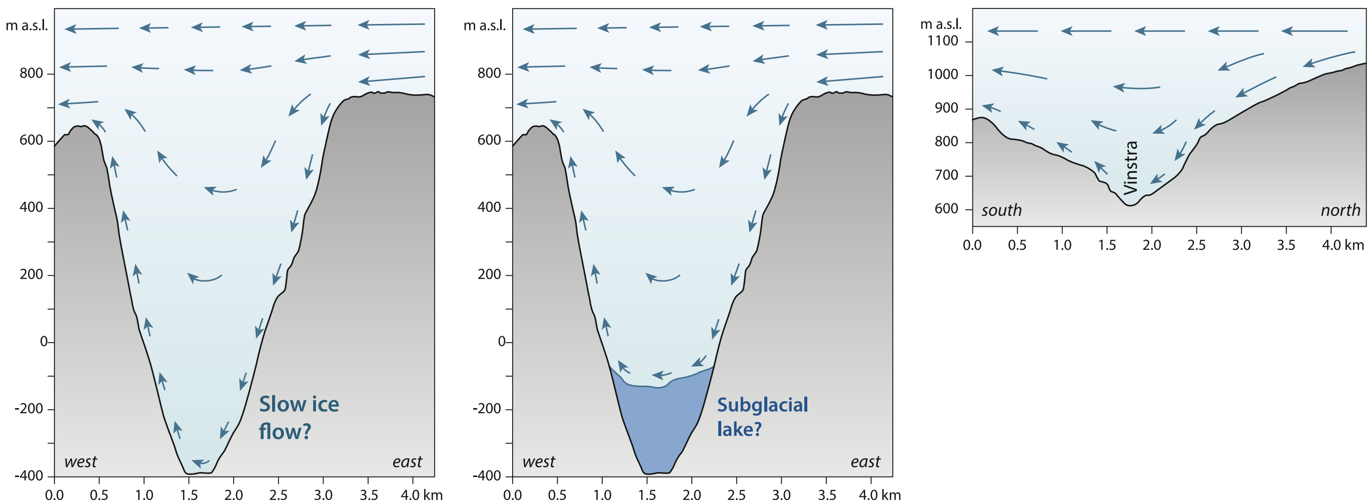

Fig. 19. Cross section of Veafjorden in our study area and the valley Vinstradalen in eastern Norway.
A and B. The two alternative hypotheses for flow across Veafjorden; the profile line is marked in Fig. 16.
C. The valley Vinstradalen where glacial striae on the slopes and till fabrics at the very base of the valley demonstrate ice flow across the valley. All three profiles are shown on the same scale.

the flow speed at the base would have been very slow. The N–S-oriented fjords in our study area follow distinct fault or fracture zones, so bedrock structures determined their locations. However, we think that deepening of the fjords only occurred when ice flowed along them, as described for Veafjorden during the deglaciation. Such situations probably represent a major part of the Quaternary period (Porter, 1989).

5.3. Ice streams versus parallel flow

Ice streams often follow subglacial valleys and fjords, although their lateral boundaries do not necessarily coincide with changes in subglacial topography, as evidenced by numerous paleo-ice streams identified for the Laurentide Ice Sheet (Margold et al., 2015; Stokes et al., 2015). It is tempting to postulate that there were always fast-flowing ice streams in 500–1000 m deep fjords, or at least that flow followed the fjord topography. However, as described in section 4.3.2, we find that the ice flow sometimes ignored valleys, fjords and other large topographic elements when the ice was thick enough. We concluded in section 4.3.2 that, with one exception described below, there were no ice streams within our area during the period of maximum ice thickness. Certainly, when the Norwegian Channel Ice Stream was active all ice from our area contributed and flowed into this ice stream (Fig. 1). Therefore, during this time the area can be considered as an upland that was drained by a fast-flowing ice stream, but which did not have internal ice streams.

Åkesson et al. (2018) (their Fig. 3) modelled ice-flow directions and speeds in this area when the ice margin was located shortly outside the coast, a situation that is comparable to our 15,000 BP reconstruction (Fig. 10A). The flow directions in the model are generally consistent with our observations, but show greater concordance with the underlying subglacial topography, as the simulated ice flow is directed towards and along the fjords. An explanation for the deviating result might be that the model includes only sliding and not flow by internal ice deformation, leading to too slow flow across land areas.

The only observations indicating converging ice flow while the margin was located beyond the coast are a series of striae near Korsfjorden (Fig. 20). Many striae show that ice-flow crossed the peninsula and islands north of Bjørnafjorden and towards Korsfjorden. This may suggest that there was an ice stream in Bjørnafjorden, which crossed over and followed Korsfjorden (Fig. 20). Such an assumption is supported by the fact that the oldest striae along Korsfjorden are converging slightly towards the fjord. An ice stream with this configuration is also found in the model simulation by Åkesson et al. (2018).

Ice flow started to follow the fjords immediately after the YD-Holocene transition, as a response to a regional lowering of the ice surface. We found that the ice margin retreated faster in the fjords than on adjacent land areas, which led to steepening of the ice surface near the margin and induced faster flow further up-fjord. During these phases, there must have been well-defined ice streams or outlet glaciers along the fjords, but because the ice margin was retreating fast, each phase was short-lived.

5.4. Calving bays and ice remnants on land

A concave ice front, with an almost radial pattern of ice flow directed towards a calving bay, is often formed in deep fjords as a semi-stable feature in a stable climate or as a retreating front during deglaciation (Gjessing, 1953, Strõmberg, 1989). The pattern of glacial striae shows that a retreating calving bay was formed in the eastern part of Korsfjorden during the Bølling-Allerød deglaciation (Fig. 20). The pattern is clearest on the northern side of the fjord where the oldest striae are parallel with the fjord, whereas younger striae point progressively towards the fjord. This change in flow direction is seen even on the nearest mountain summit on Sotra, and is especially pronounced near sea level on the south-eastern corner of Sotra where the youngest striae point towards S and SSE (Fig. 20). The preservation of the older striae suggests that withdrawal was too fast for the ice to erase all of them. On the islands between Bjørnafjorden and Korsfjorden, glacial striae point towards Korsfjorden. These directions could also be a result of the retreating calving bay, but as discussed in section 5.3 we consider that the pattern more likely shows the flow of an earlier ice stream.

A post-YD, distinct retreating calving bay is identified from the striae patterns in the part of Byfjorden that is directed towards SW (south of Askøy, Fig. 21). This part of the fjord is about 300 m deep and the oldest striae are parallel with the fjord with directions pointing towards the YD moraine, whereas younger striae on both shores show flow towards the fjord and indicate that a calving bay

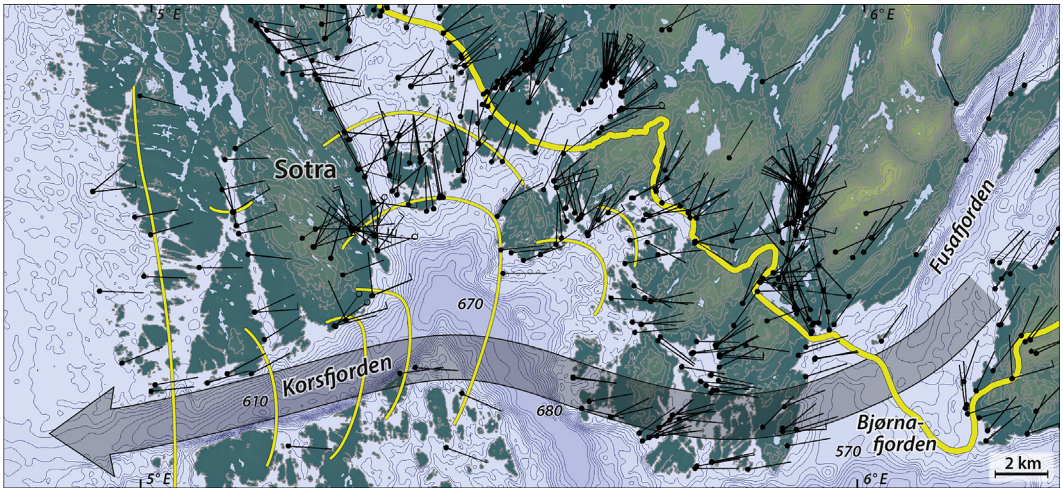

Fig. 20. A possible ice stream and calving bay in Korsfjorden. The broad grey arrow shows the possible ice stream position during periods of thick ice. The thin yellow lines mark the pattern of the ice margin during retreat. (For interpretation of the references to colour in this figure legend, the reader is referred to the Web version of this article.)

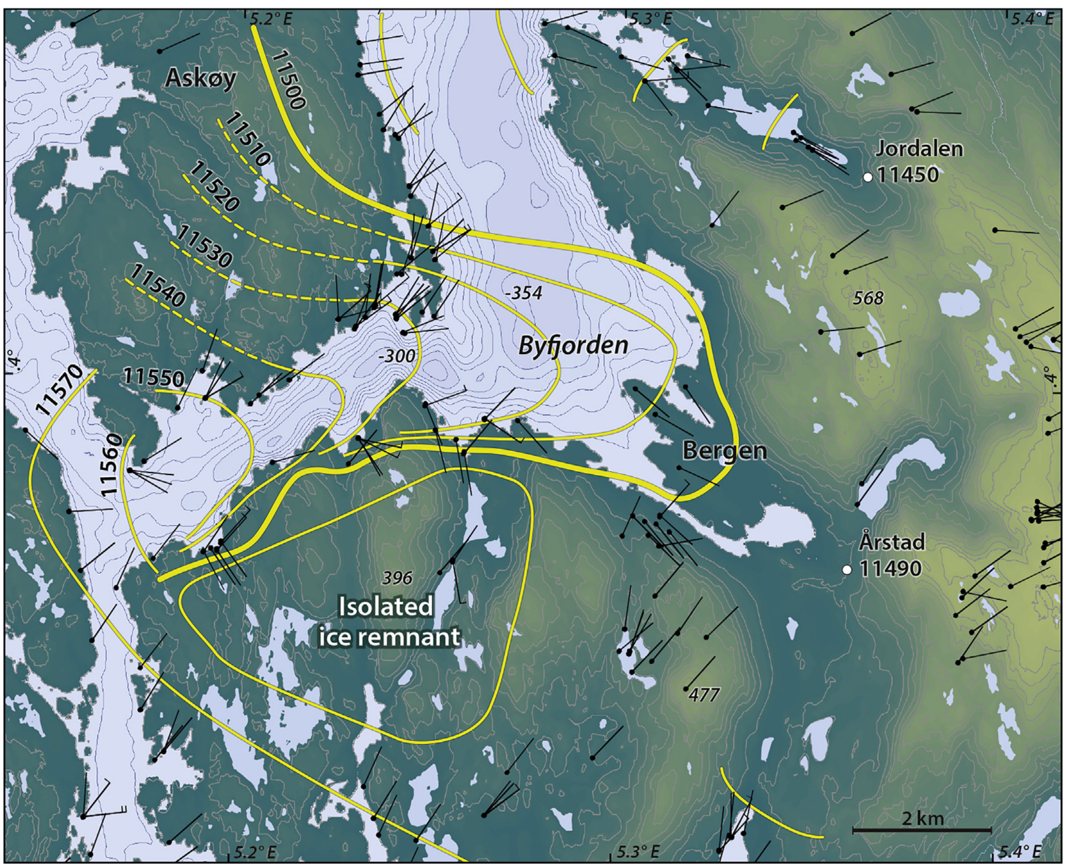

Fig. 21. The calving bay in Byfjorden. A simplified, tentative 11,500 BP ice margin position is marked with a thick line. The forms of the ice margin during retreat are marked with thin lines for each 10 years.

developed during retreat. The north-directed striae on the southern shore are especially interesting because here there is no local upland source for ice, and at this stage ice flowed towards NW in the Bergen Valley, effectively cutting off a dynamic connection with the ice sheet. Our interpretation is that the ice margin must have retreated so fast in Byfjorden that an isolated remnant of ice was left on the low-lying land south of the fjord (Fig. 21). This ice was thick enough to flow towards the fjord at right angles to the flow direction of only 2-3 decades earlier. However, as shown in section 5.1, such ice did not survive for more than a few decades (see Fig. 17).

The interpretation of very fast retreat in Byfjorden, based on the pattern of striae, is supported by the age 11,490 BP for the terrace at Årstad in the city of Bergen, which shows that the ice margin retreated 18 km, from the YD moraine (11,600 BP) to Bergen, in 60 years; a retreat rate of 160 m a^{-1}. By postulating nearly constant retreat rate, we could construct the ice-margin positions for every 10 years (Fig. 21). This means that it took only about 40 years for the ice margin in the fjord to retreat along this part of Byfjorden (Fig. 21). We regard it fascinating that the dynamics of such a fast retreat can be documented in detail by glacial striae.

Similar evidence, namely that ice left on narrow and low-lying land still could flow and produce glacial striae, is found in several places. For example at Hauglandsosen, Askøy (Fig. 22), the youngest striae are directed north, i.e. towards Herdlafjorden. This section of Askøy is a lowland cut by a number of inlets and it is only about 3 km wide. Any remnant ice separated from the main ice sheet after it retreated must have been even narrower due to retreat of the western flank. Nevertheless, this tiny chunk of ice was thick enough to flow at right angles to the previous direction and engrave glacial striae on resistant bedrock. Another example is Rosslandspollen, on the opposite side of Herdlafjorden (Fig. 4 and Fig. S1), where again the youngest striae are directed perpendicular to the fjord. The northwest flowing ice on Osterøy, described in section 4.3.6 (Fig. 16), is a good example of a large ice mass on land where flow directions changed 90° due to fast ice-margin retreat in adjacent fjords.

We have fewer observations along Fensfjorden, but the available striae show that the youngest ice flow was towards the fjord from both sides, suggesting that ice broke up in the fjord first. Fensfjorden is 500–700 m deep with no threshold located inside of the YD moraine. Our reconstruction shows that both Fensfjorden and Osterfjorden were ice free before 11,400 BP (Fig. 11B). From that time, these ice-free fjords efficiently cut off any ice flow towards the large Lindås Peninsula and adjacent islands. Although we have few observations, the youngest striae clearly suggest that a large body of ice became isolated from the main ice sheet as deglaciation progressed (Fig. 11B).

5.5. Influence of fjord morphology on retreat rates

Both the pattern of striae and calculated retreat rates show that the ice retreat was fastest in deep fjords, which is also demonstrated by several earlier studies (Stokes et al., 2014, and references therein). Distal to the YD moraines we have only studied two deep fjords. The first is Korsfjorden (section 5.4) where the development of a calving bay suggests faster retreat within the fjord than on the bordering land. In the second, the S–N-oriented Hjeltefjorden, the pattern was very different as almost all observed striae point towards the west, suggesting that the ice margin kept the S–N configuration when retreating across both the western islands and the fjord, although most striae on the eastern shore might be of YD age. Only in the very southern part of Hjeltefjorden are there some few striae suggesting flow along the fjord. Hjeltefjorden and a part of Byfjorden (section 4.3.6) are the only fjords in our study area where the most recent ice flow did not adjust to the fjord direction.

An interesting observation is that we find almost no difference in striae directions across the YD moraine, meaning that the flow pattern and ice-margin configuration were similar during the retreat of the ice margin during the Allerød and the subsequent YD re-advance.

In the area between the Herdla Moraine and the 11,300 BP ice margin the youngest striae almost everywhere are directed towards the deep fjords, showing that the ice retreated faster in the fjords than on adjacent land and shallower areas. In order to obtain a general retreat rate across the landscape, we measured retreat rates along the reconstructed YD flow lines (Fig. 10B). From the Herdla Moraine to the 11,300 BP line the retreat rate was about 120 m a^{-1}.

We have been able to compare local retreat rates in deep fjords and shallow inlets in two areas for the first 100 years of deglaciation after the YD-Holocene transition. In 400-500 m-deep Fusafjorden the retreat rate was 160 m a^{-1}, whereas in the parallel Os Valley, where water depths were less than 60 m (the marine limit), the retreat rate was only 60 m a^{-1}. The retreat rate was 160 m a^{-1} in the 200–350-m deep Byfjorden (section 5.4), whereas it was only 80 m a^{-1} in the adjacent shallow district from Fanafjord to Elveneset (section 4.3.5, Fig. 14). In the deep Fensfjorden the minimum retreat rate was 160 m a^{-1} from 11,600 to 11,400 BP.

In summary, for our area, retreat rates in the deep fjords were

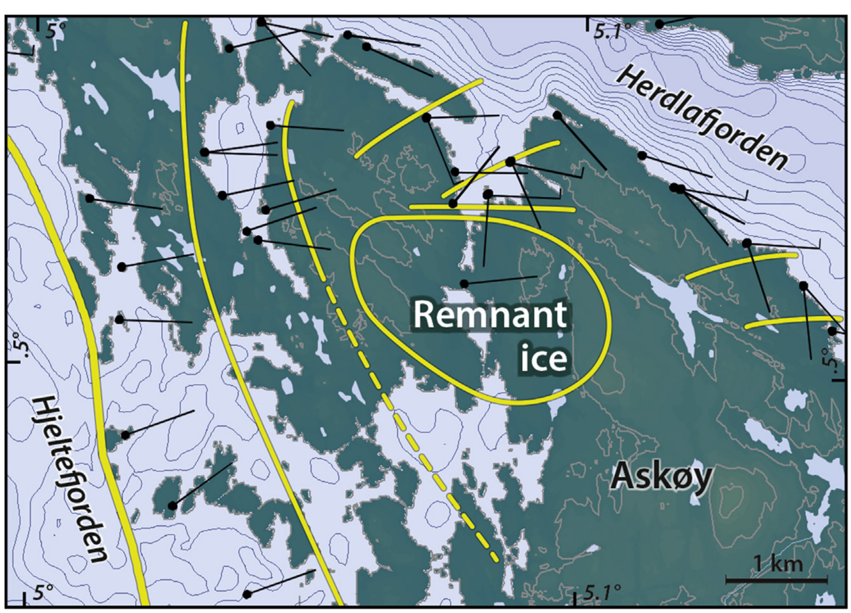

Fig. 22. Remnant ice on Askøy. The westernmost yellow line represents the Herdla Moraine, the others show the ice-margin pattern during retreat. Around Hauglandsosen, an inlet from Herdlafjorden, the northwest and north-directed striae show that the last ice must have been a small remnant on Askøy. (For interpretation of the references to colour in this figure legend, the reader is referred to the Web version of this article.)

about of 160 m a^{-1} and 60–80 m a^{-1} in shallow inlets. The average across the entire landscape was 120 m a^{-1} for the first 300 years of the Holocene. These retreat rates are high compared with rates found for fjords in other areas (Briner et al., 2009; Hughes et al., 2012; Stokes et al., 2014; Young et al., 2011), a fact even more striking when including the rates 240 and 340 m a^{-1} for Hardangerfjorden and Sognefjorden respectively (Mangerud et al., 2013). We interpret such high retreat rates as reflecting the pronounced climatic amelioration that occurred at the start in the Holocene, when temperature in this area “jumped” from nearly peak cold ice-age conditions during the YD to almost present-day-conditions within a few decades.

5.6. Synthesis of the deglaciation after the Younger Dryas

Here we give a synthesis and overview interpretation of the deglaciation of the area as a whole. The main pattern of retreat is broadly speaking similar to that reconstructed by Aa and Mangerud (1981), but our reconstruction is based on more ice-flow observations and a much improved and precise chronology.

Retreat commenced immediately after the YD/Holocene climatic boundary and was fast from the beginning, which indicates an abrupt, almost step-like, rise in summer temperatures. This glacial response is consistent with a number of stratigraphical observations in western Norway and adjacent seas showing an abrupt and large-amplitude climate warming at the YD/Holocene boundary (Birks and Birks, 2008; Eldevik et al., 2014; Haflidason et al., 1995; Paus, 1989). We assume that the warming first led to increased melting and thinning across the low-lying areas of the ice sheet, leading to grounded ice margins in the fjords becoming afloat, which further triggered sustained calving and fast retreat in the deep fjords. Melting of the underside of the floating glacier tongues by intruding warm Atlantic Water would have further enhanced melting and retreat at these sections of the ice margin. We think that the high retreat rates (160 m a^{-1}) in the deep fjords suggest that calving dominated over surface melting along the fjords at this time.

Thinning of the ice sheet, driven by retreat of the margin, forced the ice flow to follow fjords and valleys, as shown by the changing directions of glacial striae. This process propagated up-flow as the surface was further lowered by a combination of melting and further drawdown (Pritchard et al., 2009). The last ice flow was almost everywhere very topographically controlled.

The pattern and orientation of the fjords played an important role directing the course of the deglaciation. When deep fjords oriented perpendicular to the average ice-flow direction were deglaciated, they split the flank of the ice sheet leaving behind ice masses on islands or peninsulas isolated from the main ice sheet (section 5.4). Such ice masses melted away quickly, probably within a few decades (section 5.1), and thus accelerated the total rate of the deglaciation. A similar example is the Inner-Bergen-Arc Valley (Bergen City), where the ice margin retreated from both ends of the valley (Fig. 21). When considering an even larger geographical area, a similar process isolated the entire study area as the ice-margin retreated even faster in Hardangerfjorden and Sognefjorden (Mangerud et al., 2013), bounding the study area to the south and north. This strongly influenced both the ice-flow directions and rates of retreat (section 4.3.8).

Retreat slowed down and possibly even paused for a period, in the interval 11,300–11,100 BP. One factor that may have contributed to this halt in ice-margin retreat is that the margin was located in fewer and much narrower and shallower fjords, thus decreasing overall calving rates. Another factor is the Preboreal Oscillation, a cooling event dated to about 11,300–11,150 BP recorded from several places in Northern Europe and adjacent seas (Björck et al., 1997). In the Netherlands, there are indications of a more humid climate during this period (Bos et al., 2007); if there was more precipitation also in our region this would have contributed to ice growth. The midpoint of the Preboreal Oscillation is dated to 11,500–11,400 ice-core years b2k (before AD 2000) in the Greenland ice cores (Rasmussen et al., 2007), i.e. apparently slightly earlier than our reconstructed retreat deceleration. However, Rasmussen et al. (2007) use the age of 11,700 b2k for the YD/Holocene boundary. Regardless of the absolute age, the mentioned midpoint occurred 200–300 years after the onset of the Holocene in the Greenland cores, which transferred to our time scale of 11,600 BP for the YD/Holocene boundary, would be 11,350–11,250 BP. In Greenland ice cores the Preboreal Oscillation ended about 400 years after the YD/Holocene boundary (Rasmussen et al., 2007), corresponding to 11,200 BP in our scale. Thus, the age of the halt in our mapped ice-margin retreat corresponds almost exactly with the age of the Preboreal Oscillation as dated both in Europe and on Greenland and we therefore postulate that this climatic cooling caused the recorded halt in the ice-margin retreat, although the halt was favoured also by the change in topographic configuration.

Of special interest are results that were obtained from the marine core Troll 8903, collected in the Norwegian Channel only 65 km offshore our study area (Fig. 1) (Haflidason et al., 1995). Here, foraminifera show a warming of about 5 °C during a brief period that lasted only about 10 years at the YD/Holocene boundary. This event was caused by inflow of warm Atlantic Water that abruptly replaced the much colder Arctic Water, consistent with the rapid onset of the fast ice-margin retreat that we reconstruct in the present paper. Furthermore, Haflidason et al. (1995) found a distinct sea-surface temperature reversal that they correlated with the Preboreal Oscillation of the GRIP ice core.

During the maximum ice sheet extent, ice-flow was directed almost E-W across the entire area (Fig. 10A), flowing from the main ice divide towards the North Sea. During deglaciation the main flow pattern changed, with an increasing N–S component. In the final phase, an ice cap located on the mountain plateaux between our study area and Sognefjorden was separated from the main ice sheet to the east. This was partly a result of the fast retreat in deep fjords, in particular the early break-up of ice in Hardangerfjorden and Sognefjorden. However, the pattern also reflects that this mountain plateau became an accumulation area when ELA was only slightly lower than at present.

The total picture shows that the flank of the Scandinavian Ice Sheet over western Norway was very sensitive to climate change; there was a major retreat during the mild Bølling-Allerød interstadials, a correspondingly large re-advance during the YD and very fast deglaciation during the early Holocene when ice disappeared from all lowland and most mountainous areas within 700 years. Similar fluctuations have been described slightly further north in western Norway for Dansgaard-Oeschger periods 30,000–40,000 BP (Mangerud et al., 2010). At 10,900 BP, when the ice margin had retreated to the upper part of Modalen (Fig. 13) and to the heads of Hardangerfjorden and Sognefjorden (Mangerud et al., 2013), the ice sheet still covered major low-land parts of Sweden and Finland in the east (Hughes et al., 2016; Stroeven et al., 2016), suggesting a very skewed deglaciation of the ice sheet.

6. Conclusions

- The Scandinavian Ice Sheet flowed independent of valleys and fjords and at right angles to several hundred m-deep fjords in western Norway when the ice sheet was thick.
- We can date the deglaciation from 11,600 (the Younger Dryas/Holocene transition) to 10,900 BP in some areas with decadal

precision, using a well-dated shoreline diagram and elevations of preserved ice-marginal terraces.

- The pattern of retreat was deduced from analyses of 2900 glacial striae showing that the last ice flow in most places was towards deep fjords from adjacent higher ground.
- Ice masses, 2–10 km in diameter, were isolated on islands and peninsulas because the ice in the surrounding fjords broke up very fast. This process speeded up the deglaciation.
- The retreat rate was about 160 m a^{-1} in deep (300–700 m) fjords, and 60–80 m a^{-1}in shallower (<80 m) fjords.
- The mean retreat rate across this dissected fjord landscape was 120 m a^{-1} for the first 200 years of the Holocene.
- The retreat halted or slowed down 11,300–11,100 BP, probably due to cooling and/or increased precipitation during the Preboreal Oscillation.
- The ice margin retreated towards a mountain plateau north of the study area and became isolated from the main ice sheet that was located to the east.

Acknowledgements

This work was supported financially by The Research Council of Norway through the project 'Eurasian Ice Sheet and Climate Interaction' (EISCLIM; NCR 229788). Eva Bjørseth skilfully finished all illustrations. The two journal reviewers, Geoffrey Corner and Mark Furze, had a number of comments that improved the manuscript.

Appendix A. Supplementary data

Supplementary data to this article can be found online at https://doi.org/10.1016/j.quascirev.2019.04.032.

References

Svendsen, J.I., Briner, J.P., Mangerud, J., Young, N.E., 2015a. Early break-up of the Norwegian Channel Ice stream during the last glacial maximum. Quat. Sci. Rev. 107, 231–242.
Aa, A.R., 1974. Isavsmeltinga I Eksingedalen Og Områda Omkring. Master thesis. Department of Geology, University of Bergen, p. 151.
Aa, A.R., Mangerud, J., 1981. Glasialgeologi og vegetasjonsinnvandring i Indre Nordhordaland, Vest-Norge (English Summary: glacial geology and immigration of vegetation in eastern Nordhordland, western Norway). Norges geologiske undersøkelse 369, 33–75.
Aarseth, I., 1971. Deglaciasjonsforløpet I Bjørnafjordområdet, Hordaland. Master Thesis. Department of Geology, University of Bergen, p. 107.
Aarseth, I., 1997. Western Norwegian fjord sediments: age, volume, stratigraphy, and role as temporary depository during glacial cycles. Mar. Geol. 143, 39–53.
Aarseth, I., Mangerud, J., 1974. Younger dryas end moraines between Hardangerfjorden and Sognefjorden, western Norway. Boreas 3, 3–22.
Åkesson, H., Morlighem, M., Nisancioglu, K.H., Svendsen, J.I., Mangerud, J., 2018. Atmosphere-driven ice sheet mass loss paced by topography: insights from modelling the south-western Scandinavian Ice Sheet. Quat. Sci. Rev. 195, 32–47.
Andreassen, L.M., Elvehøy, H., Kjøllmoen, B., Engeset, R.V., Haakensen, N., 2005. Glacier mass-balance and length variation in Norway. Ann. Glaciol. 42, 317–325.
Anundsen, K., Simonsen, A., 1967. Et pre-borealt breframstøt på Hardangervidda og i området mellom Bergensbanen og Jotunheimen. Årbok for Universitetet i Bergen. Matematisk-naturvitenskapelige serie 7, 1–42.
Becker, L.W.M., Sejrup, H.P., Hjelstuen, B.O., Haflidason, H., Dokken, T.M., 2017. Ocean-ice sheet interaction along the SE Nordic Seas margin from 35 to 15 ka BP. Mar. Geol. 402, 99–117.
Benn, D.I., Evans, D.J.A., 1998. Glaciers and Glaciation. Arnold, London.
Bergersen, O., Garnes, K., 1972. Ice movements and till stratigraphy in the Gudbrandsdalen area. Preliminary results. Norsk Geografisk Tidsskrift 26, 1–16.
Birks, H., Birks, H., 2008. Biological responses to rapid climate change at the Younger Dryas-Holocene transition at Kråkenes, western Norway. Holocene 18, 19–30.
Björck, S., Rundgren, M., Ingólfson, Ó., Funder, S., 1997. The Preboreal oscillation around the Nordic Seas: terrestrial and lacustrine responses. J. Quat. Sci. 12, 455–465.
Bondevik, S., Mangerud, J., 2002. A calendar age estimate of a very late Younger Dryas ice sheet maximum in western Norway. Quat. Sci. Rev. 21, 1661–1676.
Bos, J.A.A., van Geel, B., van der Plicht, J., Bohncke, S.J.P., 2007. Preboreal climate oscillations in Europe: wiggle-match dating and synthesis of Dutch high-resolution multi-proxy records. Quat. Sci. Rev. 26, 1927–1950.
Briner, J.P., Bini, A.C., Anderson, R.S., 2009. Rapid early Holocene retreat of a Laurentide outlet glacier through an Arctic fjord. Nat. Geosci. 2, 496–499.
Eldevik, T., Risebrobakken, B., Bjune, A.E., Andersson, C., Birks, H.J.B., Dokken, T.M., Drange, H., Glessmer, M.S., Li, C., Nilsen, J.E.Ø., Otterå, O.H., Richter, K., Skagseth, Ø., 2014. A brief history of climate – the northern seas from the Last Glacial Maximum to global warming. Quat. Sci. Rev. 106, 225–246.
Fossen, H., Pedersen, R.-B., Bergh, S., Andresen, A., 2008. Creation of a mountain chain. In: Ramberg, I., Bryhni, I., Nøttvedt, A., Rangnes, K. (Eds.), The Making of a Land - Geology of Norway. Norsk Geologisk Forening, Trondheim, pp. 178–231.
Garnes, K., 1973. Till Studies in the Gudbrandsdalen Area, Eastern Central Norway, vol. 5. Bulletin Geological Institute, University of Uppsala, pp. 81–92.
Garnes, K., Bergersen, O., 1977. Distribution and genesis of tills in central south Norway. Boreas 6, 135–147.
Gjessing, J., 1953. Skuringsanalyse til belysning av isrecessionen ved Oslofjorden. Norsk Geografisk Tidsskrift 14, 77–99.
Haflidason, H., Sejrup, H.-P., Klitgaard Kristensen, D., Johnsen, S., 1995. Coupled response of the late glacial climatic shifts of NW-Europe reflected in Greenland ice cores: evidence from the northern North Sea. Geology 23, 1059–1062.
Hamborg, M., 1979. Deglasiasjonsforløpet I Samnager Og Kvam, Hordaland. Master Thesis. Department of Geology, University of Bergen, p. 144.
Hamborg, M., 1983. Strandlinjer og isavsmeltning i midtre Hardanger, Vest-Norge. Norges geologiske undersøkelse 387, 39–70.
Hamborg, M., Mangerud, J., 1981. En rekonstruksjon av isbevegelser under siste istid i Samnanger og Kvam, Hordaland, Vest-Norge (with English summary: a reconstruction of ice movement directions during the late Weichselian in Samnanger and Kvam, Hordaland, western Norway). Norges geologiske undersøkelse 369, 77–98.
Hughes, A.L.C., Rainsley, E., Murray, T., Fogwill, C.J., Schnabel, C., Xu, S., 2012. Rapid response of Helheim Glacier, southeast Greenland, to early Holocene climate warming. Geology 40, 427–430.
Hughes, A.L.C., Gyllencreutz, R., Lohne, Ø.S., Mangerud, J., Svendsen, J.I., 2016. The last Eurasian ice sheets – a chronological database and time-slice reconstruction, DATED-1. Boreas 45, 1–45.
IPCCP, 2014. Climate Change 2014: Synthesis Report. Contribution of Working Groups I, II and III to the Fifth Assessment Report of the Intergovernmental Panel on Climate Change. IPCCP, Geneva.
Kleman, J., 1990. On the use of glacial striae for reconstruction of paleo-ice sheet flow patterns. Geogr. Ann. 72A, 217–236.
Kleman, J., Hättestrand, C., Borgström, I., Stroeven, A., 1997. Fennoscandian palaeoglaciology reconstructed using a glacial geological inversion model. J. Glaciol. 43, 283–299.
Kolderup, C.F., 1908. Bergensfeltet og tilstødende trakter i senglacial og postglacial tid. Bergens Museum Aarbog 14 (1907), 1–266.
Kolderup, C.F., Kolderup, N.-H., 1940. Geology of the Bergen Arc system. Bergens Museums Skrifter 20, 1–137.
Ljungner, E., 1930. Spaltentektonik und Morphologie der schwedischen Skagerak-Küste. Teil III. Die Erosionsformen, vol. 21. Bulletin of the Geological Institution of the University of Upsala, pp. 255–478.
Lohne, Ø., Bondevik, S., Mangerud, J., Schrader, H., 2004. Calendar year age estimates of Allerød - younger Dryas sea-level oscillations at Os, western Norway. J. Quat. Sci. 19, 443–464.
Lohne, Ø.S., Bondevik, S., Mangerud, J., Svendsen, J.I., 2007. Sea-level fluctuations imply that the Younger Dryas ice-sheet expansion in western Norway commenced during the Allerød. Quat. Sci. Rev. 26, 2128–2151.
Lohne, Ø.S., Mangerud, J., Svendsen, J.I., 2012. Timing of the younger dryas glacial maximum in western Norway. J. Quat. Sci. 27, 81–88.
Lohne, Ø.S., Mangerud, J., Birks, H.H., 2013. Precise 14C ages of the Vedde and Saksunarvatn ashes and the Younger Dryas boundaries from western Norway and their comparison with the Greenland Ice Core (GICC05) chronology. J. Quat. Sci. 28, 490–500.
Lohne, Ø.S., Mangerud, J., Birks, H.H., 2014. IntCal13 calibrated ages of the Vedde and Saksunarvatn ashes and the younger dryas boundaries from Kråkenes, western Norway. J. Quat. Sci. 29, 506–507.
Mangerud, J., 1965. Dalfyllinger i noen sidedaler til Gudbrandsdalen, med bemerkninger om norske mammutfunn (English summary: drift in some tributary valleys of Gudbrandsdalen (Central Norway), with remarks on the Norwegian mammoth finds). Nor. Geol. Tidsskr. 45, 199–226.
Mangerud, J., 1970. Late Weichselian vegetation and ice-front oscillations in the Bergen district, western Norway. Norsk Geografisk Tidsskrift 24, 121–148.
Mangerud, J., 1986. Spor etter istider og mellomistider. In: Fossen, A.B. (Ed.), Bergensernes Fjellverden. Hardanger Forlag, Bergen, pp. 12–20.
Mangerud, J., Skreden, S., 1972. Fossil ice wedges and ground wedges in sediments below till at Voss, western Norway. Nor. Geol. Tidsskr. 52, 73–96.
Mangerud, J., Sønstegaard, E., Sejrup, H.-P., Haldorsen, S., 1981. A continuous Eemian-Early Weichselian sequence containing pollen and marine fossils at Fjøsanger, western Norway. Boreas 10, 137–208.
Mangerud, J., Andersen, S.T., Berglund, B.E., Donner, J.J., 1974. Quaternary stratigraphy of Norden, a proposal for terminology and classification. Boreas 3, 109–128.
Mangerud, J., Gulliksen, S., Larsen, E., 2010. ^{14}C-dated fluctuations of the western flank of the Scandinavian Ice Sheet 45-25 kyr BP compared with Bølling-Younger Dryas fluctuations and Dansgaard-Oeschger events in Greenland. Boreas 39, 328–342.
Mangerud, J., Gyllencreutz, R., Lohne, Ø., Svendsen, J.I., 2011. Glacial history of

Norway. In: Ehlers, J., Gibbard, P., Hughes, P. (Eds.), Quaternary Glaciations - Extent and Chronology. Elsevier, Amsterdam, pp. 279–298.
Mangerud, J., Goehring, B.M., Lohne, Ø., Svendsen, J.I., Gyllencreutz, R., 2013. Collapse of marine-based outlet glaciers from the Scandinavian ice sheet. Quat. Sci. Rev. 67, 8–16.
Mangerud, J., Aarseth, I., Hughes, A.L.C., Lohne, Ø.S., Skår, K., Sønstegaard, E., Svendsen, J.I., 2016. A major re-growth of the Scandinavian ice sheet in western Norway during Allerød-younger dryas. Quat. Sci. Rev. 132, 175–205.
Mangerud, J., Briner, J.P., Goslar, T., Svendsen, J.I., 2017. The Bølling-age Blomvåg Beds, western Norway: implications for the Older Dryas glacial re-advance and the age of the deglaciation. Boreas 46, 162–184.
Margold, M., Stokes, C.R., Clark, C.D., Kleman, J., 2015. Ice streams in the Laurentide Ice Sheet: a new mapping inventory. J. Maps 11, 380–395.
Morén, B.M., Sejrup, H.P., Hjelstuen, B.O., Borge, M.V., Schäuble, C., 2018. The last deglaciation of the Norwegian Channel – geomorphology, stratigraphy and radiocarbon dating. Boreas 47, 347–366.
Mæland, P., 1963. Kvartærgeologiske Studier I Området Mellom Granvin Og Voss. Master Thessis. Department of Geology, University of Bergen, p. 140.
Olsen, T.N., 1977. Kvartærgeologi med anvendte vurderinger av hoveddalens løsmasser, i området fra og med Eikefet-Eikemo til og med Modalen, og sentrale deler av Stølsheimen, Nordhordland. Master thesis. Department of Geology, University of Bergen, p. 109.
Ottesen, D., Dowdeswell, J.A., Rise, L., 2005. Submarine landforms and reconstruction of fast-flowing ice streams within a large Quaternary ice sheet: the 2500-km-long Norwegian-Svalbard margin (57^0-80^0N). GSA Bulletin 117, 1033–1050.
Ottesen, D., Stokes, C.R., Bøe, R., Rise, L., Longva, O., Thorsnes, T., Olesen, O., Bugge, T., Lepland, A., Hestvik, O.B., 2016. Landform assemblages and sedimentary processes along the Norwegian Channel Ice stream. Sediment. Geol. 338, 115–137.
Paus, A., 1989. Late Weichselian vegetation, climate, and floral migration at Liastemmen, North Rogaland, south-western Norway. J. Quat. Sci. 4, 223–242.
Porter, S., 1989. Some geological implications of average Quaternary glacial conditions. Quarternary Research 32, 245–261.
Pritchard, H.D., Arthern, R.J., Vaughan, D.G., Edwards, L.A., 2009. Extensive dynamic thinning on the margins of the Greenland and Antarctic ice sheets. Nature 461, 971–975.
Rasmussen, S.O., Vinther, B.M., Clausen, H.B., Andersen, K.K., 2007. Early Holocene climate oscillations recorded in three Greenland ice cores. Quat. Sci. Rev. 26, 1907–1914.
Reimer, P.J., Bard, E., Bayliss, A., Beck, J.W., Blackwell, P.G., Bronk Ramsey, C., Buck, C.E., Cheng, H., Edwards, R.L., Friedrich, M., Grootes, P.M., Guilderson, T.P., Haflidason, H., Hajdas, I., Hatté, C., Heaton, T.J., Hoffmann, D.L., Hogg, A.G., Hughen, K.A., Kaiser, K.F., Kromer, B., Manning, S.W., Niu, M., Reimer, R.W., Richards, D.A., Scott, E.M., Southon, J.R., Staff, R.A., Turney, C.S.M., van der Plicht, J., 2013. IntCal13 and Marine13 radiocarbon age calibration curves 0–50,000 Years cal BP. Radiocarbon 55, 1869–1887.
Romundset, A., Lohne, Ø.S., Mangerud, J., Svendsen, J.I., 2010. The first Holocene relative sea-level curve from the middle part of Hardangerfjorden, western Norway. Boreas 39, 87–104.
Romundset, A., Akçar, N., Fredin, O., Tikhomirov, D., Reber, R., Vockenhuber, C., Christl, M., Schlüchter, C., 2017. Lateglacial retreat chronology of the Scandinavian Ice Sheet in Finnmark, northern Norway, reconstructed from surface exposure dating of major end moraines. Quat. Sci. Rev. 177, 130–144.
Sejrup, H.P., Nygård, A., Hall, A.M., Haflidason, H., 2009. Middle and late Weichselian (Devensian) glaciation history of south-western Norway, North Sea and eastern UK. Quat. Sci. Rev. 28, 370–380.
Sejrup, H.P., Clark, C.D., Hjelstuen, B.O., 2016. Rapid ice sheet retreat triggered by ice stream debuttressing: evidence from the North Sea. Geology 44, 355–358.
Skår, K., 1975. Isavsmelting Og Postglaciale Flaumskredvifter I Arna, Hordaland. Master Thesis. Department of Geology, University of Bergen, p. 156.
Skreden, S.A., 1967. Kvartærgeologiske Undersøkelser I Området Voss-Bolstadøyri Samt Bordalen, Master Thesis. Department of Geology. University of Bergen, p. 102.
Sørensen, R., 1979. Late Weichselian deglaciation in the Oslofjord area, south Norway. Boreas 8, 241–246.
Stokes, C.R., Corner, G.D., Winsborrow, M.C.M., Husum, K., Andreassen, K., 2014. Asynchronous response of marine-terminating outlet glaciers during deglaciation of the Fennoscandian Ice Sheet. Geology 42, 455–458.
Stokes, C.R., Tarasov, L., Blomdin, R., Cronin, T.M., Fisher, T.G., Gyllencreutz, R., Hättestrand, C., Heyman, J., Hindmarsh, R.C.A., Hughes, A.L.C., Jakobsson, M., Kirchner, N., Livingstone, S.J., Margold, M., Murton, J.B., Noormets, R., Peltier, W.R., Peteet, D.M., Piper, D.J.W., Preusser, F., Renssen, H., Roberts, D.H., Roche, D.M., Saint-Ange, F., Stroeven, A.P., Teller, J.T., 2015. On the reconstruction of palaeo-ice sheets: recent advances and future challenges. Quat. Sci. Rev. 125, 15–49.
Stroeven, A.P., Hättestrand, C., Kleman, J., Heyman, J., Fabel, D., Fredin, O., Goodfellow, B.W., Harbor, J.M., Jansen, J.D., Olsen, L., Caffee, M.W., Fink, D., Lundqvist, J., Rosqvist, G.C., Strõmberg, B., Jansson, K.N., 2016. Deglaciation of Fennoscandia. Quat. Sci. Rev. 147, 91–121.
Strõmberg, B., 1989. Late Weichselian Deglaciation and Clay Varv Chronology in East-Central Sweden. Sveriges Geologiska Undersøkning, Ser. Ca 73, pp. 1–70.
Svendsen, J.I., Briner, J.P., Mangerud, J., Young, N.E., 2015b. Early break-up of the Norwegian Channel Ice stream during the last glacial maximum. Quat. Sci. Rev. 107, 231–242.
Sæle, T.H., 2017. Skuringsstriper Og Isbevegelse for Hordaland. Master Thesis. Department of Earth Science, University of Bergen, p. 110.
Vorren, T., 1977. Weichselian ice movement in South Norway and adjacent areas. Boreas 6, 247–257.
Vorren, T., Mangerud, J., 2008. Glaciations come and go. In: Ramberg, I., Bryhni, I., Nøttvedt, A., Rangnes, K. (Eds.), The Making of a Land - Geology of Norway. Norsk Geologisk Forening, Trondheim, pp. 480–533.
Young, N.E., Briner, J.P., Stewart, H.A.M., Axford, Y., Csatho, B., Rood, D.H., Finkel, R.C., 2011. Response of Jakobshavn Isbrae, Greenland, to Holocene climate change. Geology 39, 131–134.